

Accepted Manuscript

Enhancement of the tail hydrophobic interactions within the carbonic anhydrase IX active site *via* structural extension: Synthesis of novel *N*-substituted isatins-SLC-0111 hybrids as carbonic anhydrase inhibitors and antitumor agents

Wagdy M. Eldehna, Mahmoud F. Abo-Ashour, Alessio Nocentini, Radwan S. El-Haggar, Silvia Bua, Alessandro Bonardi, Sara T. Al-Rashood, Ghada S. Hassan, Paola Gratteri, Hatem A. Abdel-Aziz, Claudiu T. Supuran

PII: S0223-5234(18)30946-2

DOI: <https://doi.org/10.1016/j.ejmech.2018.10.068>

Reference: EJMECH 10854

To appear in: *European Journal of Medicinal Chemistry*

Received Date: 25 September 2018

Revised Date: 11 October 2018

Accepted Date: 31 October 2018

Please cite this article as: W.M. Eldehna, M.F. Abo-Ashour, A. Nocentini, R.S. El-Haggar, S. Bua, A. Bonardi, S.T. Al-Rashood, G.S. Hassan, P. Gratteri, H.A. Abdel-Aziz, C.T. Supuran, Enhancement of the tail hydrophobic interactions within the carbonic anhydrase IX active site *via* structural extension: Synthesis of novel *N*-substituted isatins-SLC-0111 hybrids as carbonic anhydrase inhibitors and antitumor agents, *European Journal of Medicinal Chemistry* (2018), doi: <https://doi.org/10.1016/j.ejmech.2018.10.068>.

This is a PDF file of an unedited manuscript that has been accepted for publication. As a service to our customers we are providing this early version of the manuscript. The manuscript will undergo copyediting, typesetting, and review of the resulting proof before it is published in its final form. Please note that during the production process errors may be discovered which could affect the content, and all legal disclaimers that apply to the journal pertain.

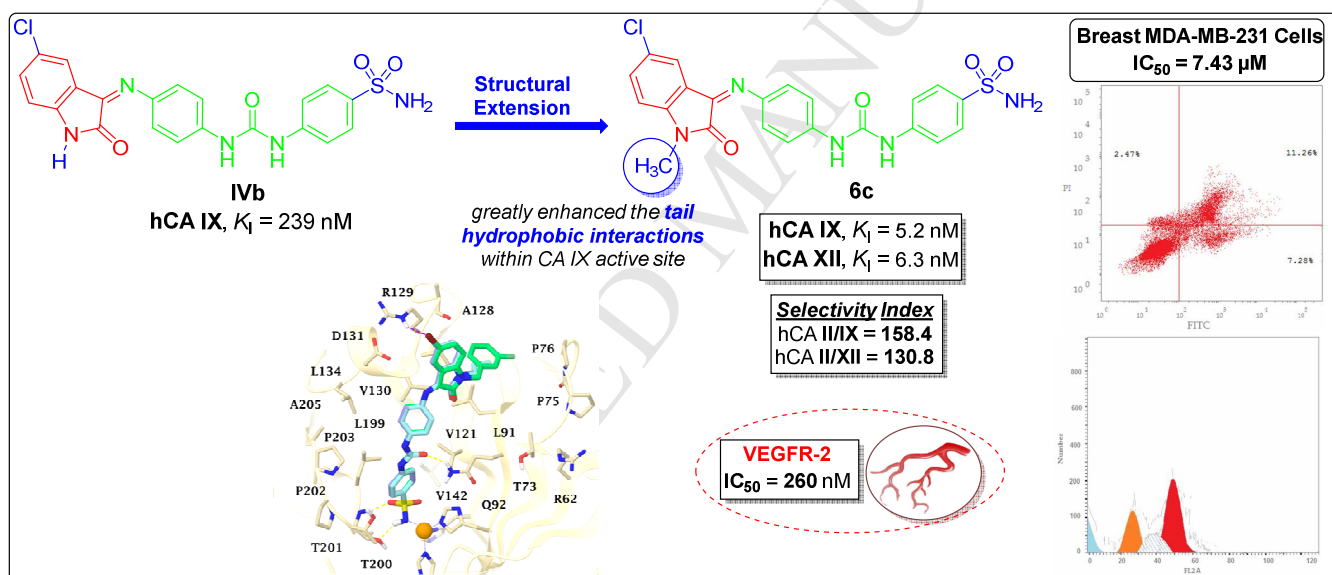


Graphical Abstract

Enhancement of the tail hydrophobic interactions within the carbonic anhydrase IX active site *via* structural extension: Synthesis of novel *N*-substituted isatins-SLC-0111 hybrids as carbonic anhydrase inhibitors and antitumor agents

Wagdy M. Eldehna*, Mahmoud F. Abo-Ashour, Alessio Nocentini, Radwan S. El-Haggag, Silvia Bua, Alessandro Bonardi, Sara T. Al-Rashood, Ghada S. Hassan, Paola Gratteri, Hatem A. Abdel-Aziz, Claudiu T. Supuran*

A substantial improvement of inhibitory profile of the target hybrids (K_{I} : 4.7–86.1 nM) towards hCA IX in comparison to *N*-unsubstituted leads **IVa-c** (K_{I} : 192–239 nM), was achieved.



Enhancement of the tail hydrophobic interactions within the carbonic anhydrase IX active site *via* structural extension: synthesis of novel *N*-substituted isatins-SLC-0111 hybrids as carbonic anhydrase inhibitors and antitumor agents

Wagdy M. Eldehna^{a,*}, Mahmoud F. Abo-Ashour^b, Alessio Nocentini^{c,d}, Radwan S. El-Haggar^e, Silvia Bua^c, Alessandro Bonardi^{c,d}, Sara T. Al-Rashood^f, Ghada S. Hassan^g, Paola Gratteri^d, Hatem A. Abdel-Aziz^h, Claudiu T. Supuran^{c,**}

^a*Department of Pharmaceutical Chemistry, Faculty of Pharmacy, Kafrelsheikh University, Kafrelsheikh, Egypt*

^b*Department of Pharmaceutical Chemistry, Faculty of Pharmacy, Egyptian Russian University, Badr City, Cairo 11829, Egypt*

^c*Department of NEUROFARBA, Section of Pharmaceutical and Nutraceutical Sciences, University of Florence, Polo Scientifico, Via U. Schiff 6, 50019, Sesto Fiorentino, Firenze, Italy*

^d*Department of NEUROFARBA, Section of Pharmaceutical and Nutraceutical Sciences, Laboratory of Molecular Modeling Cheminformatics & QSAR, University of Florence, Polo Scientifico, Via U. Schiff*

^e*Pharmaceutical Chemistry Department, Faculty of Pharmacy, Helwan University, Cairo, Egypt 6, 50019, Sesto Fiorentino, Firenze, Italy*

^f*Department of Pharmaceutical Chemistry, College of Pharmacy, King Saud University, P.O. Box 2457, Riyadh 11451, Saudi Arabia.*

^g*Department of Medicinal Chemistry, Faculty of Pharmacy, Mansoura University, Mansoura 35516, Egypt*

^h*Department of Applied Organic Chemistry, National Research Center, Dokki, Giza, P.O. Box 12622, Egypt*

ABSTRACT

Herein we report the design and synthesis of novel *N*-substituted isatins-SLC-0111 hybrids (**6a-f** and **9a-l**). A structural extension approach was adopted *via* *N*-alkylation and *N*-benzylation of isatin moiety to enhance the tail hydrophobic interactions within the carbonic anhydrase (CA) IX active site. Thereafter, a hybrid pharmacophore approach was utilized *via* merging the pharmacophoric elements of isatin and SLC-0111 in a single chemical framework. As planned, a substantial improvement of inhibitory profile of the target hybrids (K_{IS} : 4.7–86.1 nM) towards hCA IX in comparison to *N*-unsubstituted leads **IVa-c** (K_{IS} : 192–239 nM), was achieved. Molecular docking of the designed hybrids in CA IX active site unveiled, as planned, the ability of *N*-alkylated and *N*-benzylated isatin moieties to accommodate in a wide hydrophobic pocket formed by T73, P75, P76, L91, L123 and A128, establishing strong van

der Waals interactions. Hybrid **6c** displayed good anti-proliferative activity under hypoxic conditions towards breast cancer MDA-MB-231 and MCF-7 cell lines ($IC_{50} = 7.43 \pm 0.28$ and $12.90 \pm 0.34 \mu\text{M}$, respectively). Also, **6c** disrupted the MDA-MB-231 cell cycle *via* alteration of the Sub- G_1 phase and arrest of G_2 -M stage. Additionally, **6c** displayed significant increase in the percent of annexinV-FITC positive apoptotic cells from 1.03 to 18.54%. Furthermore, **6c** displayed potent VEGFR-2 inhibitory activity ($IC_{50} = 260.64 \text{ nM}$). Collectively, these data suggest **6c** as a promising lead molecule for the development of effective anticancer agents.

Keywords: Anticancer Activity; Selective hCA IX and XII inhibitors; SLC-0111 hybrids; Tail approach; VEGFR-2 inhibitors.

* Corresponding authors. E-mail addresses: wagdy2000@gmail.com (W.M. Eldehna), claudiu.supuran@unifi.it (C.T. Supuran).

1. Introduction

Carbonic anhydrases (CAs, EC 4.2.1.1) are widespread metalloenzymes in all organisms which are necessary for CO₂ hydration to bicarbonate and protons [1-3]. To date 16 diverse isoforms have been identified, which have different tissue distribution and patterns of location, thus cytosolic (I, II, III, VII, and XIII), membrane-bound (IV, IX, XII, and XIV), secreted (VI) and mitochondrial (VA and VB) forms have been described in mammals [1-3]. CAs are involved in many important physiological functions as respiration, pH regulation, ion transport, bone resorption and secretion of gastric fluid juices. So, their inhibitors became an important class of therapeutics during last decades. Some of novel applications of CAIs emerged, are topically acting antiglaucoma, anticonvulsants and antitumor agents [4-7].

On account of its limited presence in normal tissues and high overexpression in a large number of solid tumors, where it significantly contributes to survival and metastatic spread of tumor cells, hCA IX has been known as a tumor-associated protein since its discovery in the early 1990s. Thus, therapeutic strategies based on selective inhibition of CA IX have stood out as an attractive tactic for discovering therapies for several human malignancies in the current medical era [8-12]. The most exploited structural element enhances potency and selectivity of sulfonamide-like CAIs is the “tail” that the zinc-binding inhibitors incorporate [13, 14]. Several tails with a diverse chemical nature has been employed to design selective CA IX and hCA XII inhibitors [15-20].

Isatin, an endogenous compound in both human and other mammalian tissues and fluids, [21, 22], is a privileged scaffold that is endowed with diverse assortment of biological actions, to name just a few, anticancer [23-30] and CA inhibitory activities [31-38]. Interestingly, isatin scaffold has been utilized as an effective tail for the design and development of promising CAIs [31-38]. Exploring the structure activity relationships (SAR) for some reported isatin-based CAIs, (compounds **I-IV**, **Fig.1**) highlighted that *N*-alkylation or *N*-benzylation of isatin moiety could be an advantageous approach for the inhibitory activity towards hCA IX [31-34].

Incorporation of urea functionality as a linker between the zinc anchoring moiety and the tail of the inhibitor emerged as an important trend in the design of selective sulfonamide CAIs [39-45]. The most important synthesized ureido benzenesulfonamide is the clinical candidate

SLC-0111 **VI**, (**Fig. 1**), which is currently in Phase I/II clinical trials for the treatment of advanced, metastatic solid tumors [12, 45, 46]

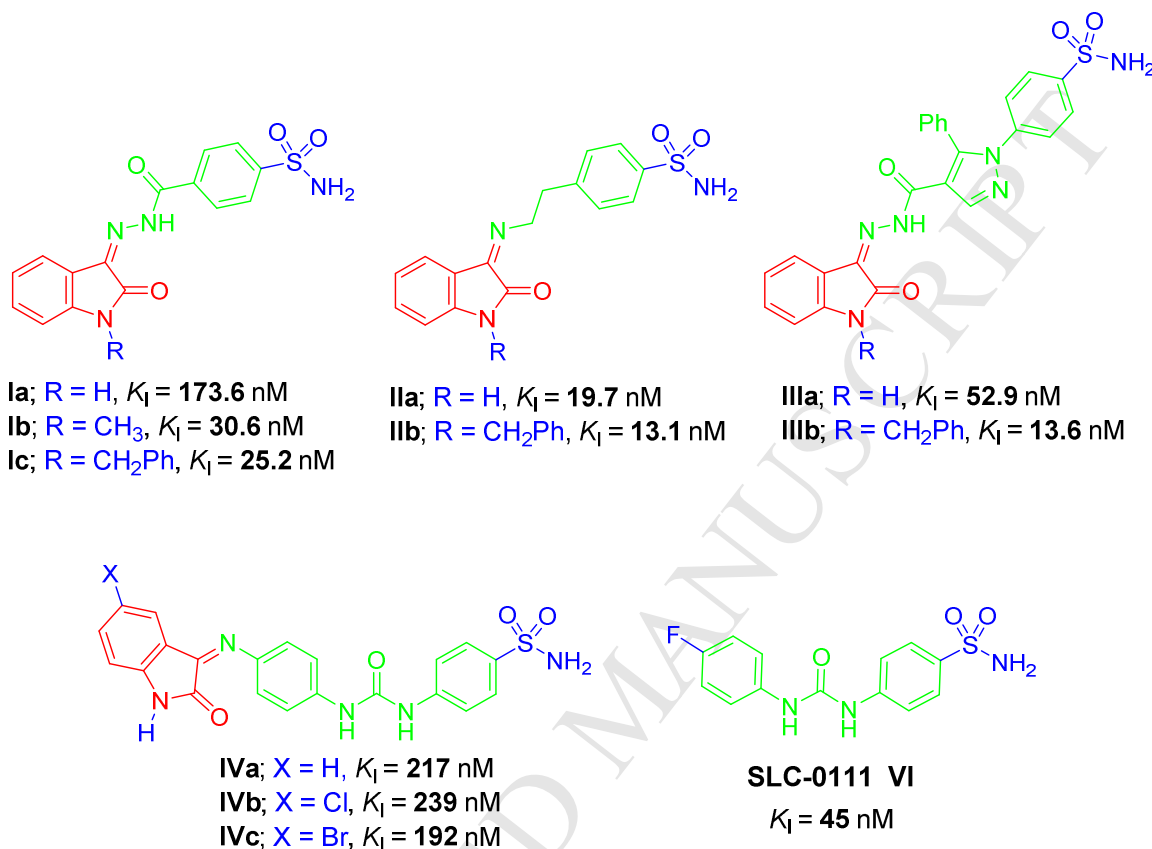


Fig. 1. Structures and K_i values against tumor-associated hCA IX isoform for some reported isatin-based (**I-V**) carbonic anhydrase inhibitors and SLC-0111.

Recently, we described a series of ureidosubstituted benzenesulfonamides incorporating isatin moieties (compounds **IVa-c**, **Fig. 1**) as CAIs. Although they displayed excellent inhibition of hCA XII in the sub- to low-nanomolar range (K_i s: 0.67 – 2.32 nM), they weakly inhibited hCA IX (K_i s: 192 – 239 nM) [37].

In light of the above findings and as a continuation of our research program to develop effective isatin-based antitumor candidates targeting the tumor-associated isoforms hCA IX and XII, it was thought worthwhile to extend our investigations around our study to improve the potency of CAIs (**IVa-c**) towards the tumor-associated isoform hCA IX and also eliminate or lower the inhibition of off-target hCA I which has a wide tissue distribution and, preferably, should not be affected in the course of anticancer drugs development.

Firstly, structural extension approach was adopted *via* *N*-alkylation and *N*-benzylation of isatin moiety to enhance the tail hydrophobic interactions within the CA IX active site. Thereafter, a hybrid pharmacophore approach was utilized *via* merging the pharmacophoric elements of isatin and SLC-0111 in a single chemical framework to synthesize two series of novel *N*-substituted isatins-SLC-0111 hybrids **6a-f** and **9a-l** (Fig. 2). Grafting halogen substituents (Cl and Br) at 5-position of the isatin tail is to ensure different lipophilic environments which could be suitable for the hydrophobic nature of the CA IX active site, and to carry out further elaboration of the target scaffold to explore a valuable SAR.

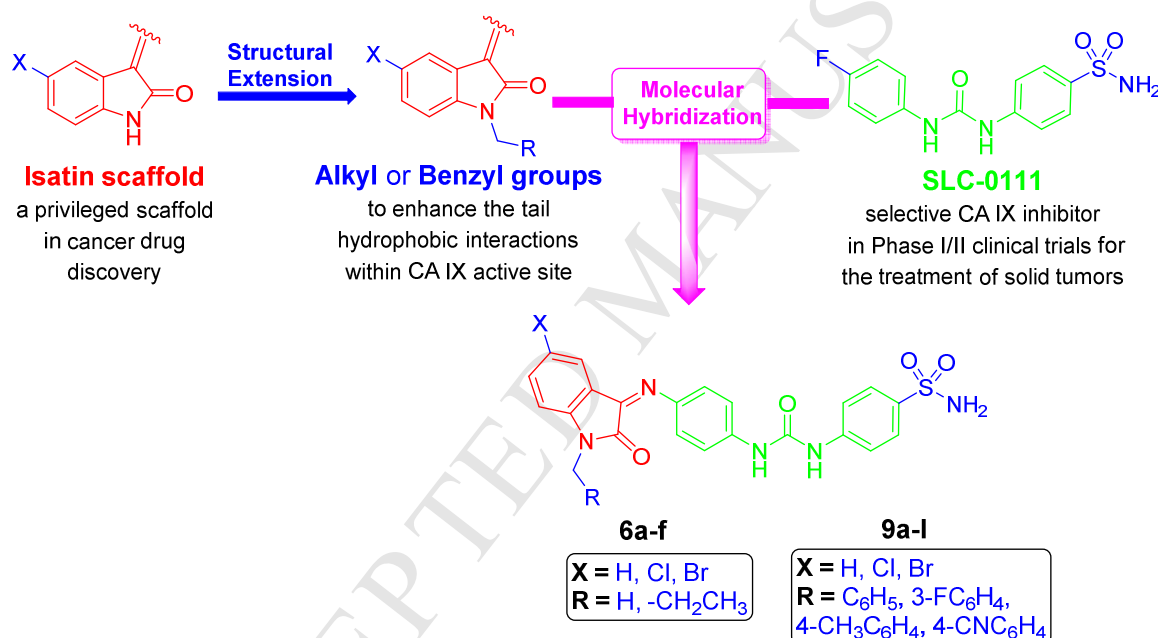


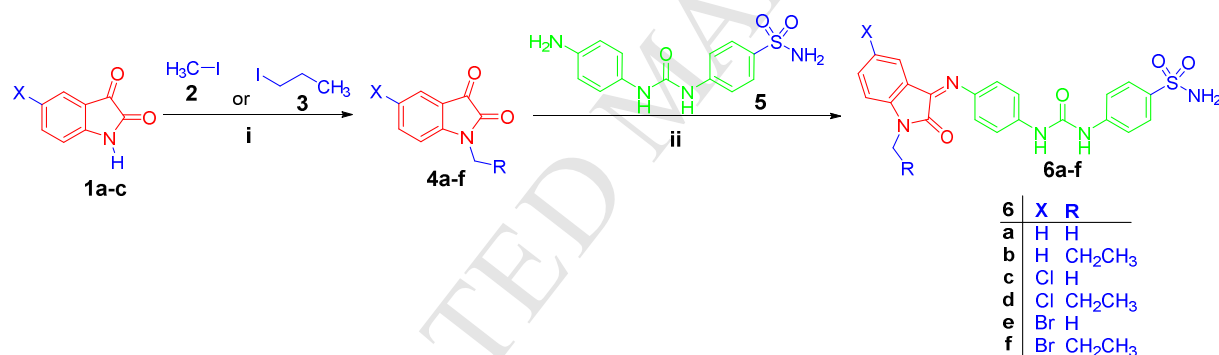
Fig. 2. Design of the target *N*-substituted isatins-SLC-0111 hybrids **6a-f** and **9a-l**.

All the synthesized hybrids **6a-f** and **9a-l** were evaluated for their CA inhibitory effects towards the physiologically relevant hCA isoforms, hCA I, II (cytosolic) as well as hCA IX and XII (transmembrane, tumor-associated isoforms) using stopped-flow CO₂ hydrase assay. Furthermore, the most potent and selective hCA IX and XII inhibitors were examined for their anti-proliferative activity towards breast cancer MDA-MB-231 and MCF-7 cell lines under hypoxic conditions. Furthermore, hybrid **6c** was examined for cell cycle disturbance and apoptosis induction in MDA-MB-231 cells. Moreover, inhibitory activity of compounds **6c**,

6d, **9c** and **9d** against VEGFR-2 were evaluated. To point out the binding modes and rationalize the trend of the inhibition profiles, molecular docking of the designed hybrids in CA II and IX active sites was carried out (PDB; 5LJT and 5FL4, respectively).

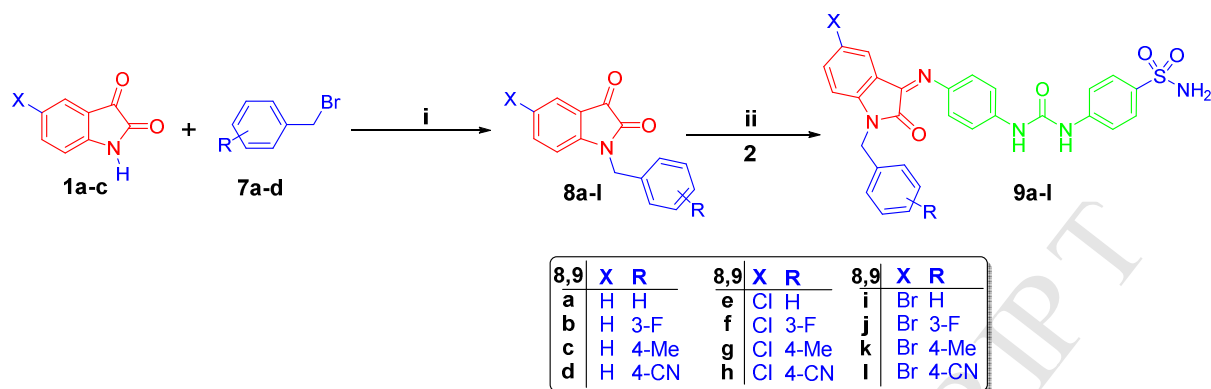
2. Results and discussion

Preparation of the new *N*-substituted isatins-SLC-0111 hybrids **6a-f** and **9a-l** in this study is illustrated in **Schemes 1** and **2**. The synthesis was initiated by *N*-alkylation of isatins **1a-c** that carried out *via* reaction with methyl iodide **2** or propyl iodide **3** in acetonitrile in the presence of potassium carbonate to furnish *N*-alkylated isatin derivatives **4a-f**. The first series of the target hybrids was obtained by condensing 4-(3-(4-aminophenyl)ureido)benzenesulfonamide **5** with the appropriate *N*-substituted isatin derivative **4a-f** in glacial acetic acid in 53-78% yield (**Scheme 1**).



Scheme 1. Synthesis of target hybrids **6a-f**; *Reagents and conditions*: (i) CH₃CN, K₂CO₃, reflux 3 h, (ii) Glacial acetic acid / reflux 3-4 h.

In **Scheme 2**, isatins **1a-c** were benzylated with different benzyl bromides **7a-d** in refluxing dry acetonitrile in the presence of potassium carbonate as a base to afford *N*-benzylated isatin derivatives **8a-l**, which subsequently were condensed with the key intermediate **5** in refluxing glacial acetic acid to produce the second group of the target hybrids **9a-l** in good yields (70-83%) (**Scheme 2**).



Scheme 2. Synthesis of target hybrids **9a-l**; *Reagents and conditions:* (i) CH₃CN, K₂CO₃, reflux 3 h, (ii) Glacial acetic acid / reflux 4-7 h.

Postulated structure of the newly synthesized hybrids **6a-f** and **9a-l** were in full agreement with their spectral and elemental analyses data.

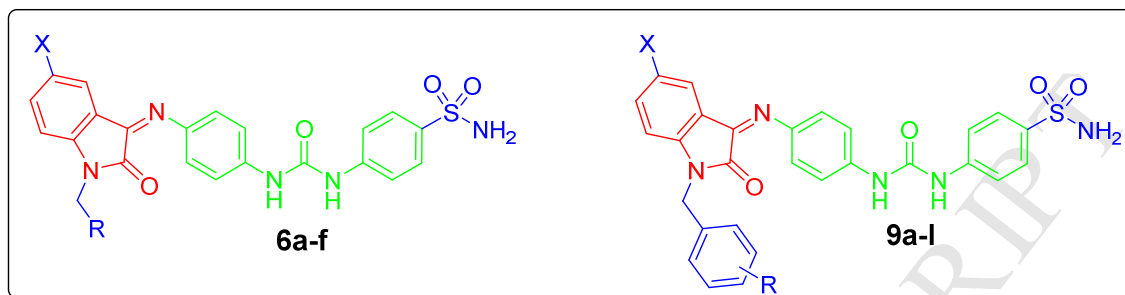
It is worth highlighting that ¹H NMR spectra of some compounds of both series (**6** and **9**) unveiled their presence as *E/Z* geometrical isomers due to the exocyclic C=N double bond. Their ¹H NMR spectra revealed two sets of signals each belonging to the *Z* and *E* isomers. The ratio between signals suggests that the *Z*-isomer is much more abundant than the *E* one (more than 70% for most compounds); however this *E/Z* ratio is NMR solvent-dependent and stable over time [37, 47]. For example, the ¹H NMR spectrum of **9a** showed two singlet signals attributable to the protons of benzylic methylene function at δ 4.86 ppm (for *E* isomer) and δ 4.97 ppm (for *Z* isomer). The integration of the latter two signals showed that the *E/Z* ratio for **9a** is 2.2:7.8.

2.2. Biological Evaluation

2.2.1. Carbonic anhydrase inhibition

The CA inhibitory effects of all the newly synthesized hybrids **6a-f** and **9a-l** were evaluated towards the physiologically relevant hCA isoforms, hCA I, II (cytosolic) as well as hCA IX and XII (transmembrane, tumor-associated isoforms) using an applied photophysics stopped-flow instrument for assaying the CA-catalyzed CO₂ hydration activity [48]. The inhibitory activities were compared to acetazolamide (AAZ), a clinically used standard CA inhibitor, and SLC-0111. The following SAR is evident from the data of **Table 1**:

Table 1. Inhibition data of human CA isoforms hCA I, II, IX and XII with SLC-0111 and hybrids **6a-f** and **9a-l**, determined by stopped-flow CO₂ hydrase assay, using acetazolamide (AAZ) as a standard drug.



Comp.	X	R	K_I (nM)*			
			hCA I	hCA II	hCA IX	hCA XII
6a	H	H	898	21.7	25.1	38.9
6b	H	CH ₂ CH ₃	939.4	9	19.6	52.2
6c	Cl	H	406.9	823.8	5.2	6.3
6d	Cl	CH ₂ CH ₃	607.2	262.3	8.2	7.8
6e	Br	H	1955.2	57.9	9.2	16.3
6f	Br	CH ₂ CH ₃	2956.1	75	26.7	9.6
9a	H	H	641.3	131.4	73.2	80.9
9b	H	3-F	2071.3	114.9	54.5	3.6
9c	H	4-CH ₃	6567.1	81.4	4.7	9.5
9d	H	4-CN	2292	77.3	9.7	8.5
9e	Cl	H	2496.4	107.5	86.1	57.4
9f	Cl	3-F	5095.8	66.6	58.8	7.7
9g	Cl	4-CH ₃	6147.9	221.5	43	50.1
9h	Cl	4-CN	8292.5	460.4	34.7	31.8
9i	Br	H	5890.7	246.4	41.2	26
9j	Br	3-F	4697	336.1	61.2	1.3
9k	Br	4-CH ₃	4638.8	440.1	26.4	58.9
9l	Br	4-CN	5842.3	611.5	36.9	16.5
SLC-0111	-	-	5080	960.0	45.0	4.5
AAZ	-	-	250	12.0	25.2	5.6

* Mean from 3 different assays, by a stopped flow technique (errors were in the range of \pm 5-10 % of the reported values).

(i) The ubiquitous cytosolic isoform hCA I was inhibited by the prepared hybrids **6a-f** and **9a-l** with K_I values ranging from 406.9 to 8292.5 nM (Table 1). Noteworthy, the *N*-alkylated derivatives **6a-f** showed a generally improved inhibitory profile towards hCA I in comparison to their *N*-benzylated counterparts **9a-l**. In particular 5-chloroisatin derivatives **6c** and **6d** displayed the best hCA I inhibitory activity with K_I values of 406.9 and 607.2 nM, respectively.

(ii) The *in vitro* kinetic data listed in Table 1 revealed that the physiologically dominant isoform hCA II was inhibited by the prepared hybrids **6a-f** and **9a-l** with inhibition constants ranging in the low-high nanomolar range, in detail, between 9 and 823.8 nM. Compound **6b** stood out as a single-digit nanomolar hCA II inhibitor that showed better activity ($K_I = 9$ nM) than the standard drug AAZ ($K_I = 12$ nM against hCA II). Moreover, hybrids **6a**, **6e**, **6f**, **9c**, **9d** and **9f** displayed good inhibitory activity against hCA II ($K_{IS} = 21.7, 57.9, 75, 81.4, 77.3$ and 66.6 nM, respectively) whereas the remaining hybrids were weak potency inhibitors (K_{IS} in the range of 107.5-823.8 nM). It is noteworthy that *N*-alkylated hybrids which incorporate C5-unsustituted isatin moiety (compounds **6a** and **6b**; $K_{IS} = 21.7$ and 9 nM, respectively) or 5-Br isatin moiety (compounds **6e** and **6f**; $K_{IS} = 57.9$ and 75 nM, respectively) displayed enhanced inhibitory activity than their *N*-benzylated analogues; compounds **9a-d** ($K_{IS}: 77.3 - 131.4$ nM) and compounds **9i-l** ($K_{IS}: 246.4 - 611.5$ nM).

(iii) The tumor-associated isoform hCA IX was efficiently inhibited by all the prepared hybrids **6a-f** and **9a-l** with K_{IS} spanning in the nanomolar range: 4.7 – 86.1 nM. Superiorly, hybrids **6c-e**, **9c** and **9d** emerged as single-digit nanomolar hCA IX inhibitors with $K_{IS} = 5.2, 8.2, 9.2, 4.7$ and 9.7 nM, respectively, which are more potent than the standard drug AAZ ($K_I = 25.2$ nM) and SLC-0111 ($K_I = 45$ nM). Also, hybrids **6a**, **6b**, **6f**, **9g-i**, **9k** and **9l** displayed better inhibitory activity ($K_{IS}: 19.6 - 43$ nM) than SLC-0111 towards hCA IX. It is noteworthy that C-5 substitution of isatin moiety elicited an impact on the inhibitory activity within the first series of derivatives (**6a-f**). Incorporation of 5-Cl isatin moiety (compounds **6c** and **6d**; $K_{IS} = 5.2$ and 8.2 nM, respectively) furnished the better inhibitory profile towards hCA IX in comparison to unsubstituted isatin-based derivatives (compounds **6a** and **6b**; $K_{IS} = 25.1$ and 19.6 nM, respectively) and 5-Br isatin-based derivatives (compounds **6e** and **6f**; $K_{IS} = 9.2$ and 26.7 nM, respectively). Investigating the impact of substitution on the benzyl group within the second series of derivatives (**9a-l**), suggested that such substitution is indispensable for hCA IX

inhibitory activities. The order of activities of the substituted benzyl members in the second series was decreased in the order of p -CH₃ > p -CN > m -F, for unsubstituted (**9b-d**) and 5-Br (**9j-k**) isatin-based derivatives. Whereas, the order of activities was decreased in the order of p -CN > p -CH₃ > m -F for 5-Cl (**9f-h**) isatin-based derivatives.

Interestingly, the adopted structural extension approach, *via* N -alkylation and N -benzylation of isatin moiety, succeed to enhance the inhibitory profile of the target hybrids (K_{IS} : 4.7 – 86.1 nM) towards hCA IX in comparison to N -unsubstituted leads **IVa-c** (K_{IS} : 192 – 239 nM) [37], as planned (**Fig. 3**).

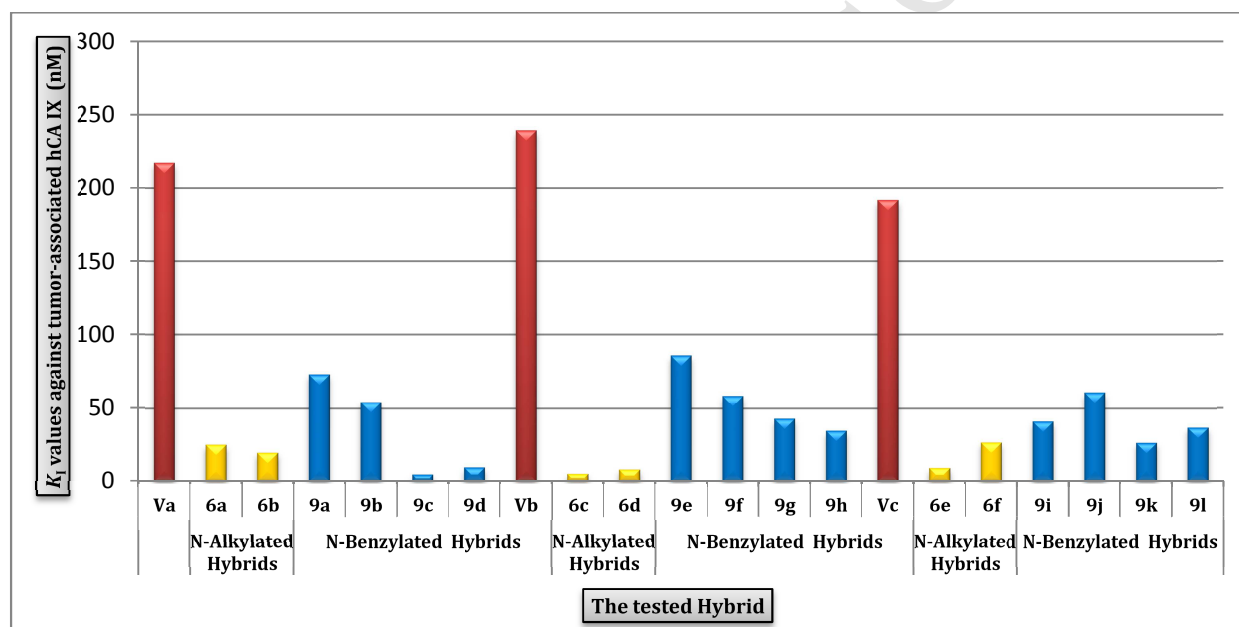


Fig. 3. K_1 values for the tested hybrids (**6a-f** and **9a-l**) and the leads **IVa-c** against tumor-associated hCA IX.

(iv) The second tumor-associated isoform tested here was hCA XII. It was obvious from the displayed results, in **Table 1**, that the newly synthesized hybrids **6a-f** and **9a-l** possessed excellent to moderate inhibitory activity against hCA XII (K_{IS} in the range of 1.3 – 80.9 nM). In particular, hybrids **9b** and **9j** were found to be more potent hCA XII inhibitors (K_{IS} = 3.6 and 1.3 nM, respectively) than AAZ (K_1 = 5.6 nM) and SLC-0111 (K_1 = 4.5 nM). Besides, compounds **6c**, **6d**, **6f**, **9c**, **9d** and **9f** displayed single-digit nanomolar activity (K_{IS} = 6.3, 7.8, 9.6, 9.5, 8.5 and 7.7 nM, respectively). As for hCA IX; substitution of the benzyl group is advantageous for hCA XII inhibitory activity, except compound **9k**. The order of hCA XII

inhibitory activities of the substituted benzyl members in the second series was decreased in the order of $m\text{-F} > p\text{-CN} > p\text{-CH}_3$. It is worth stressing that grafting $m\text{-F}$ substituent on the benzyl group (**9b**, **9f** and **9j**) resulted in a considerable improvement of the activity with 7-fold to 22-fold efficacy enhancement likened to the unsubstituted benzyl-based compound (**9a**, **9e** and **9i**).

(v) As hCA I and hCAII isozymes are physiologically relevant, the selectivity is crucial element for developing new hCA IX inhibitors. As a result of the inhibitory trends extrapolated from the data in **Table 1**, interesting selectivity index (SI) arose for most hybrids herein reported (**Table 2**). Regarding selectivity towards hCA IX over hCA II, the examined hybrids possessed good selectivity indexes spanning in the range 5.2 – 158.4, apart from non-selective hybrids **6a** and **6b** (SI = 0.9 and 0.5, respectively) and hybrids **6f**, **9a**, **9b**, **9e** and **9f** which displayed modest selectivity (SI: 1.1 – 2.8). Interestingly, all the tested hybrids **6a-f** and **9a-l** displayed interesting selectivity towards hCA IX over hCA I (SI: 8.8 – 1397.3).

Table 2. Selectivity ratios for the inhibition of hCA IX and XII over hCA I, and II for hybrids **6a-f** and **9a-l** reported in the paper, and acetazolamide.

Cpd.	Selectivity ratio			
	I/IX	II/IX	I/XII	II/XII
6a	35.8	0.9	23.1	0.6
6b	47.9	0.5	18.0	0.2
6c	78.3	158.4	64.6	130.8
6d	74.1	32	77.9	33.6
6e	212.5	6.3	120.0	3.6
6f	110.7	2.8	307.9	7.8
9a	8.8	1.8	7.9	1.6
9b	38.0	2.1	575.4	31.9
9c	1397.3	17.3	691.3	8.6
9d	236.3	8.0	269.7	9.1
9e	29.0	1.3	43.5	1.87
9f	86.7	1.1	661.8	8.7
9g	143.0	5.2	122.7	4.4

9h	239.0	13.3	260.8	14.5
9i	143.0	6.0	226.6	9.5
9j	76.8	5.5	3613.1	258.5
9k	175.7	16.7	78.8	7.5
9l	158.3	16.6	354.08	37.1
AAZ	9.9	0.5	44.6	2.2

2.2.2. *In vitro* anti-proliferative activity towards breast cancer

Breast cancer is the most frequently diagnosed malignancy among women, and the second leading cause of cancer-related deaths in women. It is considered to be a diverse group of diseases with different intrinsic tumor subtypes that have several treatment modalities and long-term survival probabilities. It is well established that hCA IX is highly expressed in breast malignancies, where numerous studies correlated the high hCA IX levels with prognosis and therapy outcomes for breast cancer patients [6, 49].

Hybrids **6c**, **6d**, **9c** and **9d** displayed single-digit nanomolar inhibitory activities towards hCA IX (K_{IS} : of 4.7 – 9.7 nM) and hCA XII (K_{IS} : of 6.3 – 9.5 nM), also they possessed good selectivity towards hCA IX over hCA I (SI: 74.1 – 1397.3) and hCA II (SI: 8 – 158.4). Accordingly, the four hybrids were selected to be examined for their anti-proliferative activity towards two breast cancer MDA-MB-231 and MCF-7 cell lines, under hypoxia conditions utilizing the MTT colorimetric assay as described by T. Mosmann [50]. A chemically-induced hypoxia was established by the use of cobalt (II) chloride hexahydrate ($\text{CoCl}_2 \cdot 6\text{H}_2\text{O}$) as a chemical inducer of HIF-1 α . The results were expressed as median growth inhibitory concentration (IC_{50}) values that represent the compound concentration required to produce a 50% inhibition of cell growth after 48 h of incubation, compared to the untreated controls (**Table 3**).

Table 3. *In vitro* anti-proliferative activity of hybrids **6c**, **6d**, **9c** and **9d** against breast MDA-MB-231 and MCF-7 cancer cell lines.

Comp.	IC ₅₀ (μM) ^a	
	MDA-MB-231	MCF-7
6c	7.43 ± 0.28	12.90 ± 0.34
6d	25.59 ± 1.17	7.36 ± 0.19
9c	48.93 ± 1.66	11.79 ± 0.82
9d	23.16 ± 1.02	5.97 ± 0.16
Dox.	8.50 ± 0.24	6.32 ± 0.21

^a IC₅₀ values are the mean ± S.D. of three separate experiments.

The results of the MTT assay displayed in **Table 3** revealed that the examined compounds generally exhibited better anti-proliferative activity towards MCF-7 cell line (IC₅₀ range: 5.97 ± 0.16 – 12.90 ± 0.34 μM) than MDA-MB-231 cells, except compound **6c** which displayed higher potency towards MDA-MB-231 cells (IC₅₀ = 7.43 ± 0.28 μM) than MCF-7 cells (IC₅₀ = 12.90 ± 0.34 μM). Concerning activity against MDA-MB-231 cells, compound **6c** emerged as the most potent counterpart, whereas, the remaining derivatives **6d**, **9c** and **9d** exhibited moderate anti-proliferative activity with IC₅₀ values equal 25.59 ± 1.17, 48.93 ± 1.66 and 23.16 ± 1.02 μM, respectively.

Interestingly, hybrid **6c** displayed dual anti-proliferative activity towards both MDA-MB-231 and MCF-7 cancer cell lines, in addition, it exhibited interesting selectivity towards hCA IX over hCA I (SI = 78.3), hCA IX over hCA II (SI = 158.4), hCA XII over hCA I (SI = 64.6) and XII over hCA II (SI = 130.8). Thence, hybrid **6c** was selected for further biological evaluations to acquire mechanistic insights into the anti-proliferative activity of the target hybrids.

2.2.3. Cell Cycle Analysis

In the current study, hybrid **6c** was assessed for its impact on the cell cycle distribution in MDA-MB-231 cells (**Fig. 4**). The results of the DNA flow cytometric analysis highlighted that treatment of MDA-MB-231 cells with hybrid **6c** at its IC₅₀ concentration (7.43 ± 0.28) resulted in a significant 8.4-fold increased percentage of MDA-MB-231 cells at Sub-G₁, with concurrent significant reduction in the G₂-M phase by approximately 4.9-fold.

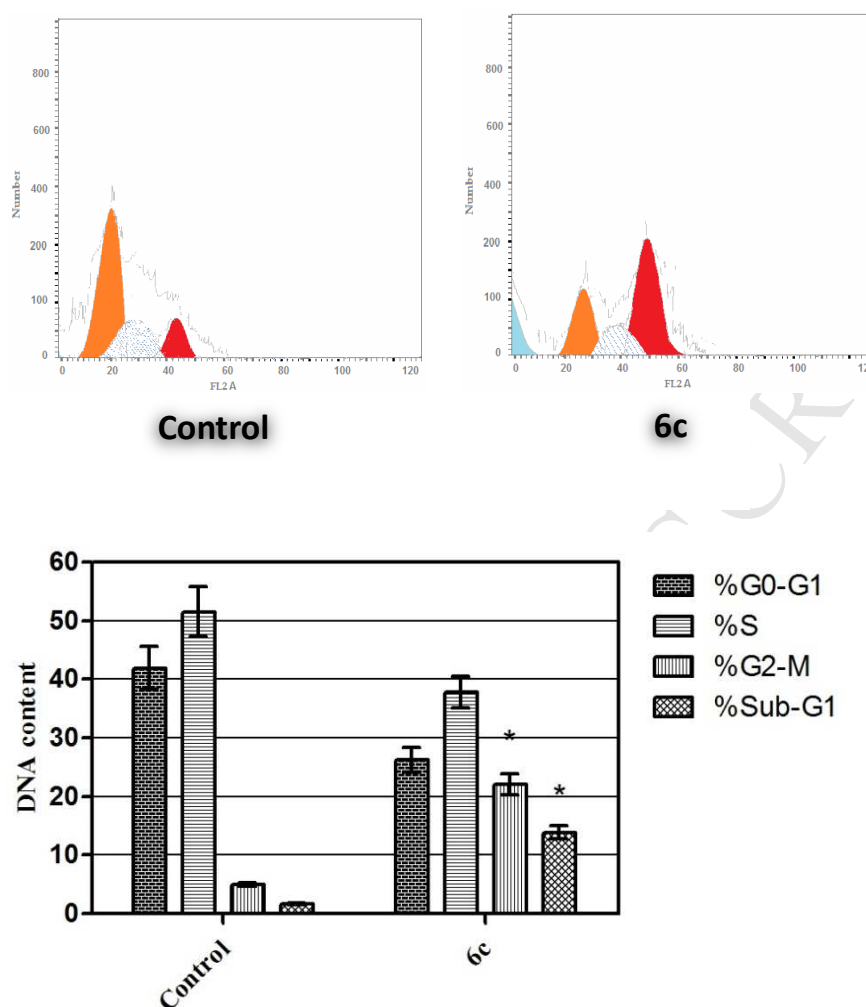


Fig. 4. Effect of hybrid **6c** on the phases of cell cycle of MDA-MB-231 cells. * Significantly different from control at $p < 0.05$. (Two-way ANOVA test).

2.2.4. AnnexinV-FITC/Propidium Iodide Analysis of Apoptosis.

AnnexinV-FITC/PI dual staining assay [51] was carried out to evaluate the effect of hybrid **6c** on both early and late apoptosis percentages in MDA-MB-231 cells (**Fig. 5, Table 4**). As presented in **Fig. 5**, the assay outcomes indicates that treatment of MDA-MB-231 cells with hybrid **6c** led to a significant increase in the percentage of annexinV-FITC-positive apoptotic cells, including both the early and late apoptotic phases (LR; from 0.77% to 7.28%, and UR; from 0.26% to 11.26%), that represents about eightfold total increase in comparison with untreated control (**Table 4**).

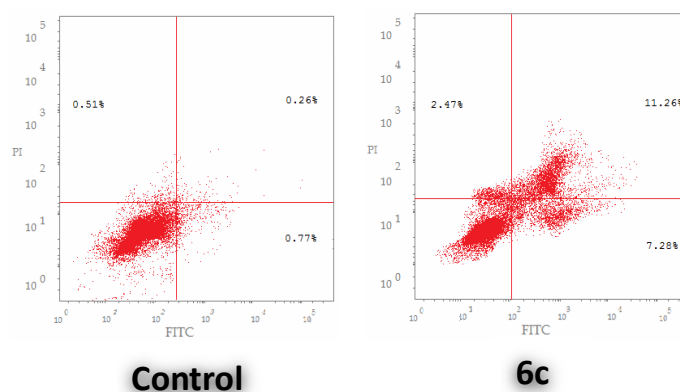


Fig. 5. Effect of hybrid **6c** on the percentage of annexin V-FITC-positive staining in MDA-MB-231 cells. The experiments were done in triplicates. The four quadrants identified as: **LL**, viable; **LR**, early apoptotic; **UR**, late apoptotic; **UL**, necrotic.

Table 4. Distribution of apoptotic cells in the AnnexinV-FITC/PI dual staining assay in MDA-MB-231 cells after treatment with hybrid **6c**.

Comp.	Early Apoptosis (Lower Right %)	Late Apoptosis (Upper Right %)	Total (L.R % + U.R %)
6c	7.28	11.26	18.54
Control	0.77	0.26	1.03

2.2.5. *In vitro* VEGFR-2 kinase inhibitory activity

On account of its significant contribution to the heterogeneity of the tumor microenvironment, hypoxia is a considerable environmental stressor that orchestrates several biological adaptations critical for cancer progression, including altered metabolism, pH regulation and angiogenesis [9].

Angiogenesis, a process of sprouting of new capillary blood vessels from the quiescent preexisting vasculature, is an important mediator of tumor progression [52]. Transcriptional activation of hypoxia inducible factor-1 α (HIF-1 α) by hypoxia leads to increased expression of several angiogenic factors that enable tumors make the angiogenic switch [9]. Members of the vascular endothelial growth factor (VEGF) family have a prevalent role among the various players involved in the angiogenesis process [53]. Accordingly, targeting tumor-associated proteins involved in pH regulation (such as CA IX and hCA XII), synchronous with targeting

proteins involved in hypoxia-induced angiogenesis (such as VEGFR-2) may furnish more effective therapeutic approach for curbing different human malignancies. Noteworthy, such dual targeting was encouraged by the previously reported good VEGFR-2 inhibitory activity of the investigated indoline urea scaffold (**IVb**; $IC_{50} = 310 \pm 40$ nM, **Table 5**) [54].

In this study, the most potent and selective hCA IX and XII inhibitors **6c**, **6d**, **9c** and **9d** were selected to evaluate their inhibitory activity against VEGFR-2 by use of a colorimetric Enzyme-Linked Immunosorbent Assay (ELISA). Sorafenib, a clinically approved VEGFR-2 inhibitor, was used as a reference drug. The results were reported as a 50% inhibition concentration values (IC_{50}) which determined as triplicate determinations from the standard curve and displayed in **Table 5**.

Table 5. IC_{50} values for the inhibitory activity of **6c**, **6d**, **9c** and **9d** against VEGFR-2.

Compound	IC_{50} (nM) ^a
	VEGFR-2
6c	260.64 ± 14.82
6d	383.61 ± 21.34
9c	462.38 ± 19.20
9d	207.04 ± 13.52
IVb ^b	310.00 ± 40.00
Sorafenib	104.01 ± 8.06

^a IC_{50} values are the mean ± SD of three separate experiments.

^b Reference [54].

Results revealed that the examined hybrids possessed VEGFR-2 inhibitory activity with IC_{50} values ranging from 207.04 to 462.38 nM. Compounds **6c** and **9d** emerged as the most potent VEGFR-2 inhibitors in this study that displayed about 2-fold decreased potency ($IC_{50} = 207.04$ and 260.64 nM) to the reference drug Sorafenib ($IC_{50} = 104.01$ nM).

Of particular interest, this study is the first to our knowledge that developed novel sulfonamides with potent and selective inhibitory activity against tumor-associated isozymes hCA IX and XII, accompanied with promising VEGFR-2 inhibitory activity.

2.3. Molecular modeling studies

To point out the binding modes and rationalize the trend of the inhibition profiles, hybrids in **Table 1** were submitted to docking within CA isozymes II and IX (PDB; 5LJT [55] and 5FL4 [56], respectively). As expected, docking solutions place the benzensulfonamide moiety of all derivatives deeply into the active site region of both the isozymes, establishing two hydrogen bonds with T199/T200 (hCA II/hCA IX). The sulfonamide negatively charged nitrogen atom directly coordinates the zinc ion and the phenyl ring is involved in several interactions with the hydrophobic region lined by V121, V143 and L198 (V121, V142, L199 in hCA IX).

In hCA II compounds bearing aliphatic portions (methyl or propyl) on the isatin nitrogen, orient differently than those substituted with benzyl groups (**Fig. 6A**). Docking poses of the first series of *N*-alkylated derivatives **6a-f** show the *N*-alkyl moiety oriented toward a little hydrophobic region defined by G132, Q136, P202, and L204. The middle phenyl ring makes hydrophobic interaction with V131, V135, L198 and P202 (**Fig. 6A**). The isatine ring is variably oriented depending on the substituent at position 5, namely a hydrogen (**6a, b**), chlorine (**6c, d**) or bromine atom (**6e, f**). The unsubstituted and chlorine bearing-hybrids orient roughly similar, but the chlorine atom of **6c** establishes unfavorable contacts with Q136 side chain that could account for the drop of its hCA II inhibition (**Table 1**). The increased hindrance of the bromine atom does not allow **6e** and **6f** to occupy the same target portion. The isatin, and in particular the middle phenyl portion of the hybrids are oriented towards P202, where the hydrophobic contacts increase significantly thus restoring the inhibition in the nanomolar range.

The size of the area described above does not allow the bulky *N*-benzylisatin tail of hybrids **9a-l** to fit inside the pocket, resulting in the budging of the entire tail toward the hydrophilic half of the cavity (**Fig. 6B**). The ureidic carbonyl group engages an H-bond with Q92 side chain and the benzyl pendants lie within the cleft formed by L57, R58, E69, D71, D72 and I91. The mainly hydrophilic nature of the pocket is not well suited for the hydrophobic characteristics of the benzyl moiety located therein and a more or less marked drop of efficacy against hCA II of these *N*-alkylated derivatives occurs (depending on the substituents on the benzyl and isatin aromatic rings, **Table 1**).

Conversely, superimposable orientations are found for all studied derivatives in hCA IX. In fact, all *N*-alkylated and *N*-benzylated isatin moieties accommodate in a wide hydrophobic pocket (devoid of hydrophilic residues instead present in the correspondent area of hCA II) formed by T73, P75, P76, L91, L123 and A128 (**Fig. 7**). As a result, the alkylation and benzoylation of the isatin NH favors the binding of these type of derivatives to hCA IX, and makes them more active towards this isoenzyme than other *N*-unsubstituted derivatives previously reported [37]. Moreover, the binding mode of halo-compounds **6c-f** and **9e-l** is strengthened by a non-conventional hydrogen bond involving R129.

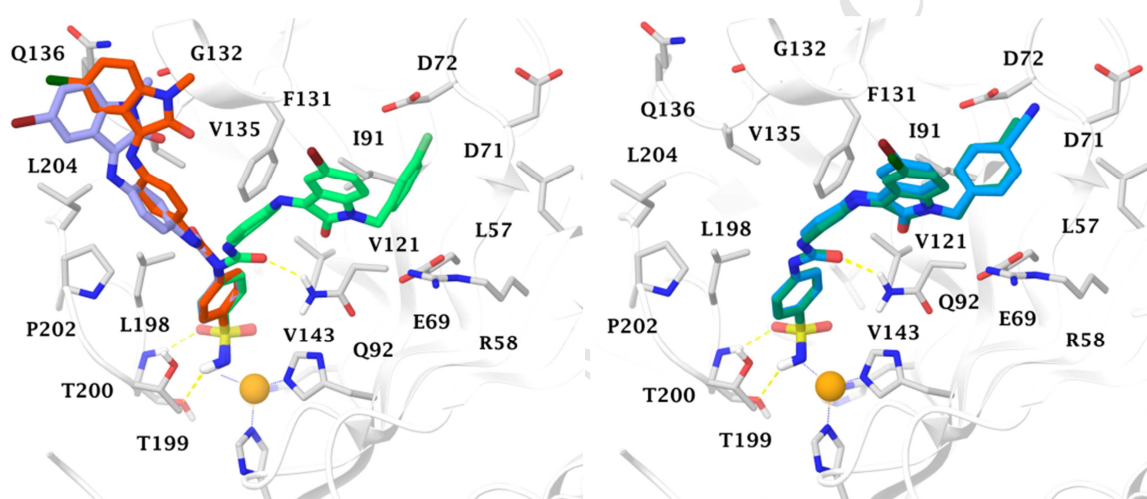


Fig. 6. Docking of A) **6c** (red), **6e** (violet) and **9j** (green), B) **9g** (green) and **9l** (blue) in hCA II.

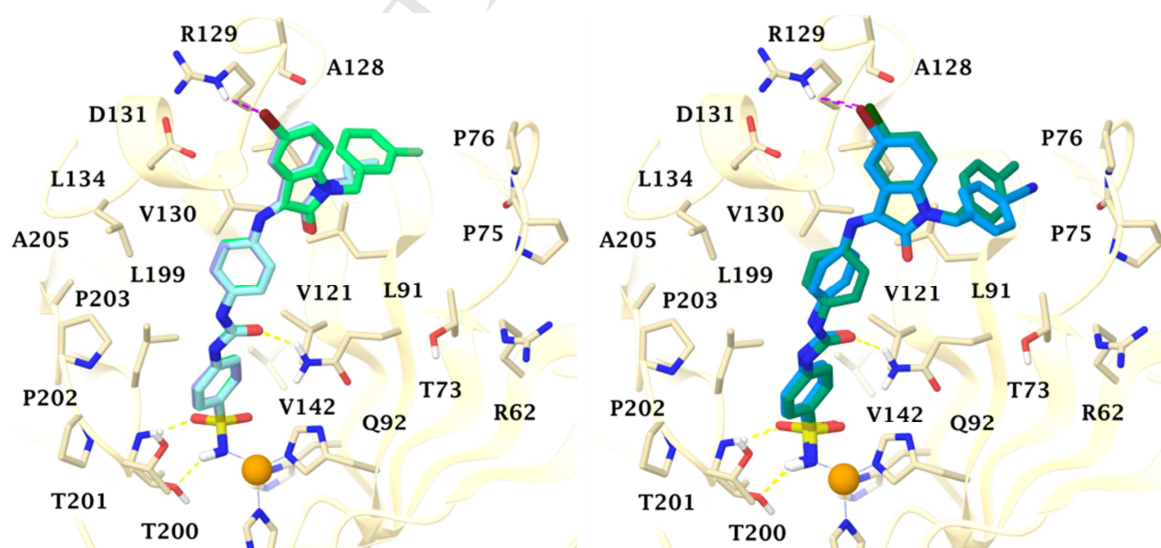


Fig. 7. Docking of A) **6d** (light blue), **6e** (violet) and **9j** (green), B) **9g** (green) and **9l** (blue) in hCA IX.

3. Conclusion

In summary, we reported the design and synthesis of two novel *N*-substituted isatins-SLC-0111 hybrids series **6a-f** and **9a-l**. A structural extension approach was adopted *via N*-alkylation and *N*-benzylation of isatin moiety to enhance the tail hydrophobic interactions within the carbonic anhydrases (CAs) IX active site. Thereafter, a hybrid pharmacophore approach was utilized *via* merging the pharmacophoric elements of isatin and SLC-0111 in a single chemical framework. The inhibition profile of the newly synthesized hybrids was determined against the physiologically relevant hCA isoforms, hCA I, II (cytosolic) as well as hCA IX and XII (transmembrane, tumor-associated isoforms) using stopped-flow CO₂ hydrase assay. Both tumor-associated isoforms hCA IX and XII were efficiently inhibited by all the prepared hybrids with *K_is* spanning in the nanomolar ranges: 4.7 – 86.1 nM and 1.3 – 80.9 nM, respectively. A significant enhancement of inhibitory activity of the target hybrids **6a-f** and **9a-l** (*K_is*: 4.7–86.1 nM) towards hCA IX in comparison to *N*-unsubstituted leads **IVa-c** (*K_is*: 192–239 nM) was achieved. Noteworthy, thirteen hybrids displayed better inhibitory activity (*K_is*: 4.7 – 43 nM) than SLC-0111 (*K_is* = 45 nM) towards hCA IX. Molecular docking of the designed hybrids in CA IX active site unveiled, as planned, the ability of *N*-alkylated and *N*-benzylated isatin moieties to accommodate in a wide hydrophobic pocket formed by T73, P75, P76, L91, L123 and A128, establishing strong van der Waals interactions. Hybrids **6c**, **6d**, **9c** and **9d**, with potent and selective IX/II inhibitory trend, were examined for their anti-proliferative activity towards breast cancer MDA-MB-231 and MCF-7 cell lines under hypoxic conditions. Compound **6c** displayed good anti-proliferative activity towards both MDA-MB-231 and MCF-7 cell lines (*IC*₅₀ = 7.43±0.28 and 12.90±0.34 μM, respectively). Furthermore, **6c** was examined for cell cycle disturbance and apoptosis induction in MDA-MB-231 cells. The results outcomes revealed the ability of **6c** to disrupt the MDA-MB-231 cell cycle *via* alteration of the Sub-G₁ phase and arrest of G₂-M stage, and its ability to increase the percent of annexinV-FITC positive apoptotic cells from 1.03 to 18.54%. Finally, hybrids **6c**, **6d**, **9c** and **9d** displayed good inhibitory activity against VEGFR-2 (*IC*₅₀: 207 – 462 nM). This study is the first to our knowledge that developed novel sulfonamides targeting tumor-associated proteins involved in pH regulation (such as CA IX and hCA XII), synchronous with targeting proteins involved in hypoxia-induced angiogenesis (such as VEGFR-2).

4. Experimental

4.1. Chemistry

4.1.1. General

Melting points were measured with a Stuart melting point apparatus and were uncorrected. Infrared (IR) Spectra were recorded as KBr disks using Shimadzu FT-IR 8400S spectrophotometer. NMR Spectra were recorded on a Varian Mercury and Bruker NMR spectrometers. ^1H spectrum was run at 400 MHz and ^{13}C spectrum was run at 100 MHz in deuterated dimethylsulfoxide ($\text{DMSO-}d_6$). Chemical shifts are expressed in values *ppm* using the solvent peak as internal standard. All coupling constant (*J*) values are given in hertz. The abbreviations used are as follows: s, singlet; d, doublet; m, multiplet. Elemental analyses were carried out at the Regional Center for Microbiology and Biotechnology, Al-Azhar University, Cairo, Egypt. Analytical thin layer chromatography (TLC) on silica gel plates containing UV indicator was employed routinely to follow the course of reactions and to check the purity of products.

4.1.2. Synthesis of compound 5

Compound **5** was prepared according to the literature procedures [57].

4.1.3. Synthesis of *N*-substituted isatin derivatives **4a-f** and **8a-l**.

Isatin derivatives **1a-c** (0.005 mol) were stirred in acetonitrile (20 mL) with (0.007 mol) of the appropriate methyl iodide **2**, propyl iodide **3** or benzyl bromide **7a-d** in the presence of catalytic amount of potassium iodide with (0.010 mol) of dry potassium carbonate at reflux temperature. The reaction was monitored with TLC. After complete of reaction, the mixture was poured into ice-water, the formed solid was collected, washed with water and recrystallized from ethanol-water to furnish the final compounds **4a-f** and **8a-l**. [58-61]

4.1.3.1. 5-Bromo-1-(3-fluorobenzyl)indoline-2,3-dione **8j**

Red crystals (yield 75%); m.p. 171-173 °C; ^1H NMR ($\text{DMSO-}d_6$, 400 MHz) δ *ppm*: 4.94 (s, 2H, benzylic protons), 6.90-7.74 (m, 7H, Ar-H); ^{13}C NMR ($\text{DMSO-}d_6$, 100 MHz) δ *ppm*: 42.89

(benzylic carbon), 113.47, 114.49, 114.71, 114.92, 115.57, 120.21, 123.81, 127.12, 131.09, 138.70, 139.92, 149.38, 158.56, 161.62, 164.05, 182.11; Anal. Calcd. for C₁₅H₉BrFNO₂ (334.14): C, 53.92; H, 2.71; N, 4.19; found C, 54.07; H, 2.69; N, 4.24.

4.1.3.2. 4-((5-Bromo-2,3-dioxindolin-1-yl)methyl)benzotrile **8l**

Red crystals (yield 81%); m.p. 201-203 °C; ¹H NMR (DMSO-*d*₆, 400 MHz) δ ppm: 4.98 (s, 2H, benzylic protons), 6.89 (s, 1H, Ar-H), 7.57-7.98 (m, 6H, Ar-H); ¹³C NMR (DMSO-*d*₆, 100 MHz) δ ppm: 42.64 (benzylic carbon), 112.03, 113.36, 115.59, 119.17, 120.36, 127.10, 130.21, 131.10, 131.80, 132.79, 137.51, 139.85, 149.18, 158.70 (N-CO-CO-), 182.01 (N-CO-CO-); Anal. Calcd. for C₁₆H₉BrN₂O₂ (341.16): C, 56.33; H, 2.66; N, 8.21; found C, 56.21; H, 2.68; N, 8.17.

4.1.4. Synthesis of target compounds **6a-f** and **9a-l**.

The key intermediate **2** was refluxed with equivalent amount of different isatin derivatives **4a-f** or **8a-l** in glacial acetic acid. The reaction was monitored with TLC. After complete of the reaction, the formed solid was collected and washed with water and recrystallized from DMF/ethanol to get the target compounds **6a-f** and **9a-l** respectively.

4.1.4.1. 4-{3-[4-((1-Methyl-2-oxindolin-3-ylidene)amino)phenyl]ureido}benzenesulfonamide **6a**.

Orange powder (yield 73%); m.p. over 280 °C; IR (KBr, ν cm⁻¹): 3123-3400 broad band (NH, NH₂), 1724, 1612 (2C=O), 1307, 1150 (SO₂); ¹H NMR (DMSO-*d*₆, 400 MHz) δ ppm: 3.10, 3.19 (s, 3H, N-CH₃), 6.68 (d, 1H, Ar-H, *J*=8 Hz), 6.81 (t, 1H, Ar-H, *J*=8 Hz), 6.96 (d, 2H, Ar-H, *J*=8.4 Hz), 7.09 (d, 1H, Ar-H, *J*=7.6 Hz), 7.19 (s, 2H, NH₂, D₂O exchangeable), 7.41 (t, 1H, Ar-H, *J*=7.6 Hz), 7.54-7.62 (m, 4H, Ar-H), 7.71 (d, 2H, Ar-H, *J*=8.4 Hz), 8.88, 8.92 (s, 1H, NH, D₂O exchangeable), 9.08, 9.10 (s, 1H, NH, D₂O exchangeable); Anal. Calcd. for C₂₂H₁₉N₅O₄S (449.49): C, 58.79; H, 4.26; N, 15.58; found C, 58.65; H, 4.22; N, 15.67.

4.1.4.2. 4-{3-[4-((2-Oxo-1-propylindolin-3-ylidene)amino)phenyl]ureido}benzenesulfonamide **6b**.

Yellow powder (yield 70%); m.p. over 280 °C; IR (KBr, ν cm⁻¹): 3122-3395 broad band (NH, NH₂), 1724, 1610 (2C=O), 1300, 1150 (SO₂); ¹H NMR (DMSO-*d*₆, 400 MHz) δ ppm: 0.92 (t,

3H, $\text{CH}_3\text{-CH}_2$, $J=8.0$ Hz), 1.59 (m, 2H, $\text{CH}_3\text{-CH}_2$), 3.70 (t, 2H, $N\text{-CH}_2$, $J=8.0$ Hz), 6.68 (d, 1H, Ar-H, $J=7.2$ Hz), 6.81 (t, 1H, Ar-H, $J=7.6$ Hz), 7.01 (d, 2H, Ar-H, $J=8.4$ Hz), 7.16-7.23 (m, 3H, 1H Ar-H and 2H of NH_2 , D_2O exchangeable), 7.41-7.52 (m, 1H, Ar-H), 7.59-7.66 (m, 4H, Ar-H), 7.76 (d, 2H, Ar-H, $J=8.4$ Hz), 8.92 (s, 1H, NH, D_2O exchangeable), 9.12 (s, 1H, NH, D_2O exchangeable); ^{13}C NMR (DMSO- d_6 , 100 MHz) δ ppm: 11.68 (2 CH_3), 19.03, 20.5 (CH_2), 41.29, 41.50 ($N\text{-CH}_2$), 109.98, 110.71, 114.61, 115.74, 117.58, 117.98 (2C), 118.56, 119.20, 119.85, 121.82, 122.44, 122.59, 123.12, 125.34, 127.32 (2C), 134.07, 134.67, 137.37, 137.49, 137.65, 137.87, 142.98, 143.31, 144.93, 146.07, 147.68, 151.34, 152.69 (aromatic carbon), 152.79, 154.22 (C=O of urea), 157.51, 162.82 (C=O of isatin); Anal. Calcd. for $\text{C}_{24}\text{H}_{23}\text{N}_5\text{O}_4\text{S}$ (477.54): C, 60.36; H, 4.85; N, 14.67; found C, 60.51; H, 4.89; N, 14.75.

4.1.4.3. *4-{3-[4-((5-Chloro-1-methyl-2-oxoindolin-3-ylidene)amino)phenyl]ureido}benzenesulfonamide 6c.*

Orange red powder (yield 53%); m.p. over 280°C ; IR (KBr, ν cm^{-1}): 3123-3350 broad band (NH, NH_2), 1714, 1612 (2C=O), 1300, 1150 (SO_2); ^1H NMR (DMSO- d_6 , 400 MHz) δ ppm: 3.51 (s, 3H, $N\text{-CH}_3$), 6.66 (s, 1H, Ar-H), 7.02 (d, 2H, Ar-H, $J=8.4$), 7.14 (d, 1H, Ar-H, $J=7.2$ Hz), 7.23 (s, 2H, NH_2 , D_2O exchangeable), 7.47-7.56 (m, 2H, Ar-H), 7.61-7.66 (m, 3H, Ar-H), 7.75 (d, 2H, Ar-H, $J=8.8$ Hz), 8.95 (s, 1H, NH, D_2O exchangeable), 9.12 (s, 1H, NH, D_2O exchangeable); ^{13}C NMR (DMSO- d_6 , 100 MHz) δ ppm: 19.03, 26.73 ($N\text{-CH}_3$), 111.39, 112.15, 112.68, 116.84, 118.00 (2C), 118.43, 119.41, 119.75, 121.91, 123.15, 123.48, 124.20, 124.46, 126.34, 127.31, 127.43 (2C), 133.11, 133.85, 137.39, 137.93, 138.51, 142.34, 143.26, 144.30, 145.19, 147.00, 150.06, 152.64 (aromatic carbon) 152.74, 153.14 (C=O of urea), 157.43, 162.55 (C=O of isatin); Anal. Calcd. for $\text{C}_{22}\text{H}_{18}\text{ClN}_5\text{O}_4\text{S}$ (483.93): C, 54.60; H, 3.75; N, 14.47; found C, 54.83; H, 3.72; N, 14.41.

4.1.4.4. *4-{3-[4-((5-Chloro-2-oxo-1-propylindolin-3-ylidene)amino)phenyl]ureido}benzenesulfonamide 6d.*

Orange powder (yield 63%); m.p. over 280°C ; IR (KBr, ν cm^{-1}): 3113-3378 broad band (NH, NH_2), 1724, 1612 (2C=O), 1317, 1155 (SO_2); ^1H NMR (DMSO- d_6 , 400 MHz) δ ppm: 0.88 (t, 3H, $\text{CH}_3\text{-CH}_2$, $J=7.6$ Hz), 1.55 (m, 2H, $\text{CH}_3\text{-CH}_2$), 3.67 (t, 2H, $N\text{-CH}_2$, $J=7.2$ Hz), 6.64 (s, 1H, Ar-H), 7.01 (d, 1H, Ar-H, $J=8.8$ Hz), 7.14-7.25 (m, 4H, 2H Ar-H and 2H of NH_2 , D_2O

exchangeable), 7.43-7.54 (m, 2H, Ar-H), 7.57-7.69 (m, 3H, Ar-H), 7.71 (d, 2H, Ar-H, $J=8.8$ Hz), 8.95 (s, 1H, NH, D₂O exchangeable), 9.10 (s, 1H, NH, D₂O exchangeable); ¹³C NMR (DMSO-*d*₆, 100 MHz) δ ppm: 11.61 (CH₃), 20.66 (CH₂), 41.62 (N-CH₂), 111.66, 112.40, 116.94, 117.78, 117.94, 117.98, 118.39 (2C), 119.35 (2C), 119.73 (2C), 122.07, 123.17, 123.57, 124.62, 126.21, 127.28 (2C), 133.86, 137.36, 137.89, 138.52, 142.30, 143.24, 144.34, 144.65, 146.45, 150.08, 152.62 (aromatic carbon), 152.74, 153.09 (C=O of urea), 157.30, 162.49 (C=O of isatin); Anal. Calcd. for C₂₄H₂₂ClN₅O₄S (511.98): C, 56.30; H, 4.33; N, 13.68; found C, 56.47; H, 4.29; N, 13.77.

4.1.4.5. *4-{3-[4-((5-Bromo-1-methyl-2-oxoindolin-3-ylidene)amino)phenyl]ureido}benzenesulfonamide 6e.*

Orange red powder (yield 78%); m.p. over 280 °C; IR (KBr, ν cm⁻¹): 3105-3340 broad band (NH, NH₂), 1714, 1610 (2C=O), 1300, 1150 (SO₂); ¹H NMR (DMSO-*d*₆, 400 MHz) δ ppm: 3.10, 3.18 (s, 3H, N-CH₃), 6.76 (s, 1H, Ar-H), 6.99 (d, 2H, Ar-H, $J=8.4$ Hz), 7.08 (d, 1H, Ar-H, $J=8.0$ Hz), 7.19 (s, 2H, NH₂, D₂O exchangeable), 7.21 (d, 1H, Ar-H, $J=8.8$ Hz), 7.43 (d, 1H, Ar-H, $J=8.8$ Hz), 7.57-7.62 (m, 3H, Ar-H), 7.71 (d, 2H, Ar-H, $J=8.8$ Hz), 8.91, 8.96 (s, 1H, NH, D₂O exchangeable) 9.08, 9.10 (s, 1H, NH, D₂O exchangeable); Anal. Calcd. for C₂₂H₁₈BrN₅O₄S (528.38): C, 50.01; H, 3.43; N, 13.25; found C, 49.89; H, 3.45; N, 13.20.

4.1.4.6. *4-{3-[4-((5-Bromo-2-oxo-1-propylindolin-3-ylidene)amino)phenyl]ureido}benzenesulfonamide 6f.*

Red powder (yield 77%); m.p. over 280 °C; IR (KBr, ν cm⁻¹): 3123-3320 broad band (NH, NH₂), 1727, 1619 (2C=O), 1307, 1160 (SO₂); ¹H NMR (DMSO-*d*₆, 400 MHz) δ ppm: 0.88 (t, 3H, CH₃-CH₂, $J=8.0$ Hz), 1.64 (m, 2H, CH₃-CH₂), 3.64 (t, 2H, N-CH₂, $J=8.0$ Hz), 6.48 (d, 1H, Ar-H, $J=8.4$ Hz), 6.79 (s, 1H, Ar-H), 7.01-7.10 (m, 2H, Ar-H), 7.12-7.23 (m, 3H, 1H Ar-H and 2H of NH₂, D₂O exchangeable), 7.54-7.62 (m, 4H, Ar-H), 7.66-7.73 (m, 2H, Ar-H), 8.95 (s, 1H, NH, D₂O exchangeable), 9.10 (s, 1H, NH, D₂O exchangeable); ¹³C NMR (DMSO-*d*₆, 100 MHz) δ ppm: 11.64 (CH₃), 19.03, 20.68 (CH₂), 41.46, 41.65 (N-CH₂), 111.52, 112.08, 112.81, 113.93, 114.91, 117.40, 118.02 (2C), 118.41, 119.20, 119.43, 119.71, 123.31, 123.96, 124.22, 127.32 (2C), 127.45, 135.93, 136.65, 137.40, 137.95, 138.61, 142.28, 143.27, 144.34, 144.99, 146.80, 149.85, 152.64 (aromatic carbon), 152.75, 152.97 (C=O of urea), 157.19, 162.39 (C=O

of isatin); Anal. Calcd. for $C_{24}H_{22}BrN_5O_4S$ (556.44): C, 51.81; H, 3.99; N, 12.59; found C, 52.03; H, 3.95; N, 12.55.

4.1.4.7. 4-{3-[4-((1-Benzyl-2-oxoindolin-3-ylidene)amino)phenyl]ureido}benzenesulfonamide **9a**.

Red powder (yield 78%); m.p. over 280 °C; IR (KBr, ν cm^{-1}): 3127-3395 broad band (NH, NH_2), 1715, 1612 (2C=O), 1317, 1150 (SO_2); 1H NMR (DMSO- d_6 , 400 MHz) δ ppm: 4.86, 4.97 (2s, 2H, benzylic proton), 6.73 (d, 1H, Ar-H, $J=8.0$ Hz), 6.80 (t, 1H, Ar-H, $J=8.0$ Hz), 7.00-7.04 (m, 3H, Ar-H), 7.18 (s, 2H, NH_2 , D_2O exchangeable), 7.27-7.43 (m, 6H, Ar-H), 7.55-7.62 (m, 4H, Ar-H), 7.71 (d, 2H, Ar-H, $J=8.4$ Hz), 8.94, 8.98 (2s, 1H, NH, D_2O exchangeable), 9.12, 9.16 (2s, 1H, NH, D_2O exchangeable); Anal. Calcd. for $C_{28}H_{23}N_5O_4S$ (525.58): C, 63.99; H, 4.41; N, 13.33; found C, 64.17; H, 4.38; N, 13.32.

4.1.4.8. 4-{3-[4-((1-(3-Fluorobenzyl)-2-oxoindolin-3-ylidene)amino)phenyl]ureido}benzenesulfonamide **9b**.

Red powder (yield 70%); m.p. over 280 °C; IR (KBr, ν cm^{-1}): 3123-3400 broad band (NH, NH_2), 1724, 1610 (2C=O), 1300, 1160 (SO_2); 1H NMR (DMSO- d_6 , 400 MHz) δ ppm: 5.08 (s, 2H, benzylic proton), 6.73 (d, 1H, Ar-H, $J=7.2$ Hz), 6.78 (d, 1H, Ar-H, $J=8$ Hz), 6.89 (d, 1H, Ar-H, $J=8$ Hz), 6.99 (d, 2H, Ar-H, $J=8.8$ Hz), 7.14 (d, 1H, Ar-H, $J=8.4$ Hz), 7.18 (s, 2H, NH_2 , D_2O exchangeable), 7.30 (t, 1H, Ar-H, $J=7.6$ Hz), 7.38 (d, 1H, Ar-H, $J=8.8$ Hz), 7.52-7.62 (m, 4H, Ar-H), 7.67-7.73 (m, 4H, Ar-H), 8.97 (s, 1H, NH, D_2O exchangeable), 9.15 (s, 1H, NH, D_2O exchangeable); Anal. Calcd. for $C_{28}H_{22}FN_5O_4S$ (543.57): C, 61.87; H, 4.08; N, 12.88; found C, 61.75; H, 4.06; N, 12.83.

4.1.4.9. 4-{3-[4-((1-(4-Methylbenzyl)-2-oxoindolin-3-ylidene)amino)phenyl]ureido}benzenesulfonamide **9c**.

Orange powder (yield 78%); m.p. over 280 °C; IR (KBr, ν cm^{-1}): 3120-3365 broad band (NH, NH_2), 1724, 1610 (2C=O), 1307, 1160 (SO_2); 1H NMR (DMSO- d_6 , 400 MHz) δ ppm: 3.27 (s, 3H, $-CH_3$), 4.98 (s, 2H, benzylic proton), 6.71 (d, 1H, Ar-H, $J=7.2$ Hz), 6.80 (t, 1H, Ar-H, $J=7.6$ Hz), 6.98-7.10 (m, 3H, Ar-H), 7.17 (s, 2H, NH_2 , D_2O exchangeable), 7.25-7.46 (m, 5H, Ar-H), 7.54-7.67 (m, 4H, Ar-H), 7.71 (d, 2H, Ar-H, $J=8.4$ Hz), 8.97 (s, 1H, NH, D_2O exchangeable), 9.15 (s, 1H, NH, D_2O exchangeable); ^{13}C NMR (DMSO- d_6 , 100 MHz) δ ppm:

21.15, 21.75 (CH₃), 42.62, 42.78 (benzylic carbon), 110.18, 110.95, 112.12, 112.15, 116.28, 117.52, 117.99 (2C), 119.30, 119.73, 121.52, 122.30, 122.76, 122.98, 123.47, 125.30, 125.34, 127.21 (2C), 130.36, 130.45, 131.32, 131.90, 132.72, 133.90, 134.52, 137.38, 137.60, 137.85, 138.01, 138.17, 142.85, 143.32, 144.83, 145.41, 146.94, 150.99, 152.69 (aromatic carbon), 152.75, 153.90 (C=O of urea), 157.75, 163.15 (C=O of isatin); Anal. Calcd. for C₂₉H₂₅N₅O₄S (539.61): C, 64.55; H, 4.67; N, 12.98; found C, 64.72; H, 4.65; N, 13.04.

4.1.4.10. *4-{3-[4-((1-(4-Cyanobenzyl)-2-oxoindolin-3-ylidene)amino)phenyl]ureido}benzenesulfonamide 9d.*

Orange powder (yield 75%); m.p. over 280 °C; IR (KBr, ν cm⁻¹): 3123-3387 broad band (NH, NH₂), 1720, 1612 (2C=O), 1300, 1150 (SO₂); ¹H NMR (DMSO-*d*₆, 400 MHz) δ ppm: 5.08 (s, 2H, benzylic proton), 6.78 (d, 1H, Ar-H, *J*=7.2 Hz), 6.84 (t, 1H, Ar-H, *J*=7.2 Hz), 7.01-7.08 (m, 3H, Ar-H), 7.23 (s, 2H, NH₂, D₂O exchangeable), 7.36 (t, 1H, Ar-H, *J*=7.2 Hz), 7.47 (d, 1H, Ar-H, *J*=8.8 Hz), 7.58-7.66 (m, 5H, Ar-H), 7.75 (d, 3H, Ar-H, *J*=8.4 Hz), 7.95 (s, 1H, Ar-H), 8.95 (s, 1H, NH, D₂O exchangeable), 9.13 (s, 1H, NH, D₂O exchangeable); ¹³C NMR (DMSO-*d*₆, 100 MHz) δ ppm: 42.52, 42.70 (benzylic carbon), 110.18, 110.90, 112.09, 112.14, 116.22, 117.59, 117.99 (2C), 118.52, 119.12, 119.34, 119.83, 121.42, 122.25, 122.76, 122.98, 123.47, 125.36, 125.36, 127.32 (2C), 130.36, 130.42, 131.38, 131.90, 132.72, 133.90, 134.50, 137.37, 137.58, 137.80, 138.00, 138.19, 142.91, 143.30, 144.88, 145.42, 146.94, 150.99, 152.69 (aromatic carbon), 152.80, 153.99 (C=O of urea), 157.78, 163.20 (C=O of isatin); Anal. Calcd. for C₂₉H₂₂N₆O₄S (550.59): C, 63.26; H, 4.03; N, 15.26; found C, 63.37; H, 4.00; N, 15.31.

4.1.4.11. *4-{3-[4-((1-Benzyl-5-chloro-2-oxoindolin-3-ylidene)amino)phenyl]ureido}benzenesulfonamide 9e.*

Dark red powder (yield 70%); m.p. over 280 °C; IR (KBr, ν cm⁻¹): 3123-3357 broad band (NH, NH₂), 1724, 1619 (2C=O), 1304, 1150 (SO₂); ¹H NMR (DMSO-*d*₆, 400 MHz) δ ppm: 4.98 (s, 2H, benzylic proton), 6.69 (s, 1H, Ar-H), 7.04-7.07 (m, 2H, Ar-H), 7.14 (s, 2H, Ar-H), 7.18 (s, 2H, NH₂, D₂O exchangeable), 7.31-7.39 (m, 3H, Ar-H), 7.54 (d, 2H, Ar-H, *J*=8.8 Hz), 7.59-7.62 (m, 2H, Ar-H), 7.66 (d, 2H, Ar-H, *J*=8.8 Hz), 7.71 (d, 2H, Ar-H, *J*=8.8 Hz), 9.03 (s, 1H,

NH, D₂O exchangeable), 9.17 (s, 1H, NH, D₂O exchangeable); Anal. Calcd. for C₂₈H₂₂ClN₅O₄S (560.03): C, 60.05; H, 3.96; N, 12.51; found C, 60.13; H, 3.95; N, 12.47.

4.1.4.12. *4-{3-[4-((5-Chloro-1-(3-fluorobenzyl)-2-oxoindolin-3-ylidene)amino)phenyl]ureido}benzenesulfonamide 9f.*

Red powder (yield 75%); m.p. over 280 °C; IR (KBr, ν cm⁻¹): 3120-3340 broad band (NH, NH₂), 1724, 1601 (2C=O), 1307, 1170 (SO₂); ¹H NMR (DMSO-*d*₆, 400 MHz) δ ppm: : 4.96, 5.07 (s, 2H, benzylic proton), 6.78 (d, 1H, Ar-H, *J*=8.0 Hz), 6.85 (t, 1H, Ar-H, *J*=8.0 Hz), 7.02-7.09 (m, 3H, Ar-H), 7.24 (s, 2H, NH₂, D₂O exchangeable), 7.36 (t, 1H, Ar-H, *J*=8.0 Hz), 7.48 (d, 1H, Ar-H, *J*=8.0 Hz), 7.60-7.67 (m, 4H, Ar-H), 7.76 (d, 3H, Ar-H, *J*=8.0 Hz), 7.93 (d, 1H, Ar-H, *J*=8.0 Hz), 8.92, 8.95 (s, 1H, NH, D₂O exchangeable), 9.12, 9.13 (s, 1H, NH, D₂O exchangeable); ¹³C NMR (DMSO-*d*₆, 100 MHz) δ ppm: 42.83, 42.98 (benzylic carbon), 111.85, 112.58, 114.57, 114.62, 114.79, 114.81, 114.97, 115.02, 117.36, 117.99 (2C), 118.03, 118.42, 119.53 (2C), 119.76 (2C), 122.17, 123.47, 123.76, 123.79, 123.82, 123.92, 124.69, 126.64, 127.33, 127.73 (2C), 131.13, 131.18, 131.21, 131.26, 133.04, 133.74, 137.42, 138.03, 138.71, 138.98, 139.05, 139.07, 139.15, 142.29, 143.27, 144.07, 144.32, 145.82, 149.72, 152.65, 152.77, 152.88 (aromatic carbon), 157.50, 161.61 (C=O of urea), 162.81, 164.03 (C=O of isatin); Anal. Calcd. for C₂₈H₂₁ClFN₅O₄S (578.02): C, 58.18; H, 3.66; N, 12.12; found C, 58.05; H, 3.67; N, 12.09.

4.1.4.13. *4-{3-[4-((5-Chloro-1-(4-methylbenzyl)-2-oxoindolin-3-ylidene)amino)phenyl]ureido}benzenesulfonamide 9g.*

Orange powder (yield 83%); m.p. over 280 °C; IR (KBr, ν cm⁻¹): 3123-3388 broad band (NH, NH₂), 1714, 1602 (2C=O), 1300, 1150 (SO₂); ¹H NMR (DMSO-*d*₆, 400 MHz) δ ppm: 3.19 (s, 3H, -CH₃), 4.78 (s, 2H, benzylic proton), 6.49 (d, 2H, Ar-H, *J*=8.0 Hz), 6.77 (s, 0.5H, Ar-H), 7.00-7.08 (m, 3.5H, Ar-H), 7.16 (s, 2H, NH₂, D₂O exchangeable), 7.54-7.63 (m, 5H, Ar-H), 7.67-7.73 (m, 4H, Ar-H), 8.24 (s, 1H, NH, D₂O exchangeable), 8.86 (s, 1H, NH, D₂O exchangeable); Anal. Calcd. for C₂₉H₂₄ClN₅O₄S (574.05): C, 60.68; H, 4.21; N, 12.20; found C, 60.42; H, 4.18; N, 12.26.

4.1.4.14. *4-{3-[4-((5-Chloro-1-(4-cyanobenzyl)-2-oxoindolin-3-ylidene)amino)phenyl]ureido}benzenesulfonamide 9h.*

Yellow powder (yield 73%); m.p. over 280 °C; IR (KBr, ν cm^{-1}): 3120-3320 broad band (NH, NH₂), 1724, 1617 (2C=O), 1307, 1150 (SO₂); ¹H NMR (DMSO-*d*₆, 400 MHz) δ ppm: 4.96, 5.07 (2s, 2H, benzylic proton), 6.74 (s, 1H, Ar-H), 6.95 (d, 1H, Ar-H, *J*=8 Hz), 7.03 (d, 1H, Ar-H, *J*=8 Hz), 7.24 (s, 2H, NH₂, D₂O exchangeable), 7.35 (d, 1H, Ar-H, *J*=8), 7.45 (t, 1H, Ar-H, *J*=8.4 Hz), 7.56-7.67 (m, 5H, Ar-H), 7.76 (d, 4H, Ar-H, *J*=7.6 Hz), 7.94 (s, 1H, Ar-H), 8.97, 9.01 (s, 1H, NH, D₂O exchangeable), 9.12, 9.15 (s, 1H, NH, D₂O exchangeable); ¹³C NMR (DMSO-*d*₆, 100 MHz) δ ppm: 42.64, 42.80 (benzylic carbon), 111.77, 112.10, 112.15, 112.49, 117.52, 117.99, 118.03, 118.40, 119.12, 119.21, 119.54, 119.77, 122.16, 123.51, 124.08, 124.69, 126.65, 127.32, 127.73, 130.34, 130.39, 131.27, 131.31, 131.87, 131.93, 132.72, 133.00, 133.70, 137.41, 137.86, 137.94, 138.01, 138.67, 142.28, 143.26, 143.98, 144.32, 145.71, 149.78, 152.65 (aromatic carbon), 152.77, 152.93 (C=O of urea), 157.62, 162.93 (C=O of isatin); Anal. Calcd. for C₂₉H₂₁ClN₆O₄S (585.04): C, 59.54; H, 3.62; N, 14.37; found C, 59.42; H, 3.58; N, 14.35.

4.1.4.15.

4-{3-[4-((1-Benzyl-5-bromo-2-oxoindolin-3-

ylidene)amino)phenyl]ureido}benzenesulfonamide **9i**.

Dark red powder (yield 71%); m.p. over 280 °C; IR (KBr, ν cm^{-1}): 3123-3350 broad band (NH, NH₂), 1724, 1603 (2C=O), 1307, 1145 (SO₂); ¹H NMR (DMSO-*d*₆, 400 MHz) δ ppm: 4.99 (s, 2H, benzylic proton), 6.71 (s, 1H, Ar-H), 7.06-7.12 (m, 2H, Ar-H), 7.18 (s, 2H, Ar-H), 7.19 (s, 2H, NH₂, D₂O exchangeable), 7.33-7.38 (m, 3H, Ar-H), 7.56 (d, 2H, Ar-H, *J*=8.8 Hz), 7.61-7.64 (m, 2H, Ar-H), 7.68 (d, 2H, Ar-H, *J*=8.8 Hz), 7.74 (d, 2H, Ar-H, *J*=8.8 Hz), 9.05 (s, 1H, NH, D₂O exchangeable), 9.18 (s, 1H, NH, D₂O exchangeable); ¹³C NMR (DMSO-*d*₆, 100 MHz) δ ppm: 42.68, 42.82 (benzylic carbon), 111.79, 112.18, 112.21, 112.51, 117.52, 117.99, 119.18, 119.25, 119.57, 119.80, 122.19, 123.55, 124.17, 124.75, 126.65, 127.35, 127.75, 130.34, 130.45, 131.29, 131.35, 131.89, 131.92, 132.72, 133.15, 133.74, 137.43, 137.89, 137.94, 138.01, 138.69, 142.32, 143.28, 143.98, 144.37, 145.75, 149.78, 152.67 (aromatic carbon), 152.79, 152.96 (C=O of urea), 157.65, 162.97 (C=O of isatin); Anal. Calcd. for C₂₈H₂₂BrN₅O₄S (604.48): C, 55.64; H, 3.67; N, 11.59; found C, 55.73; H, 3.65; N, 11.67.

4.1.4.16.

4-{3-[4-((5-Bromo-1-(3-fluorobenzyl)-2-oxoindolin-3-

ylidene)amino)phenyl]ureido}benzenesulfonamide **9j**.

Red powder (yield 80%); m.p. over 280 °C; IR (KBr, ν cm^{-1}): 3123-3400 broad band (NH, NH₂), 1704, 1610 (2C=O), 1300, 1142 (SO₂); ¹H NMR (DMSO-*d*₆, 400 MHz) δ ppm: 4.93, 5.04 (s, 2H, benzylic proton), 6.55-7.24 (m, 8H, 2H of NH₂, D₂O exchangeable and 6H, Ar-H), 7.40-7.78 (m, 9H, Ar-H), 9.03 (s, 1H, NH, D₂O exchangeable), 9.17 (s, 1H, NH, D₂O exchangeable); ¹³C NMR (DMSO-*d*₆, 100 MHz) δ ppm: 42.95 (benzylic carbon), 112.33, 113.04, 114.32, 114.55, 114.77, 115.02, 115.28, 117.57, 117.83 (2C), 118.03, 118.41, 119.54, 119.71, 121.46, 123.49, 123.77, 124.28, 124.91, 127.32 (2C), 127.48, 131.18, 131.26, 135.86, 136.53, 137.41, 138.03, 138.71, 138.96, 139.03, 139.13, 142.27, 143.27, 144.32, 144.46, 146.18, 149.56, 152.65, 152.76, 152.79, 157.37 (aromatic carbon), 158.03, 161.60 (C=O of urea), 162.68, 164.03 (C=O of isatin); Anal. Calcd. for C₂₈H₂₁BrFN₅O₄S (622.47): C, 54.03; H, 3.40; N, 11.25; found C, 53.87; H, 3.38; N, 11.24.

4.1.4.17. *4-{3-[4-((5-Bromo-1-(4-methylbenzyl)-2-oxoindolin-3-ylidene)amino)phenyl]ureido}benzenesulfonamide 9k.*

Orange powder (yield 75%); m.p. over 280 °C; IR (KBr, ν cm^{-1}): 3129-3340 broad band (NH, NH₂), 1719, 1603 (2C=O), 1300, 1150 (SO₂); ¹H NMR (DMSO-*d*₆, 400 MHz) δ ppm: : 3.10, 3.19 (2s, 3H, -CH₃), 4.68, 4.78 (2s, 2H, benzylic proton), 6.49 (d, 2H, Ar-H, *J*=8.0 Hz), 6.63 (br s, 0.5H, Ar-H), 7.00-7.11 (m, 3.5H, Ar-H), 7.14-7.16 (m, 3H, 1H, Ar-H, 2H, NH₂, D₂O exchangeable), 7.50-7.63 (m, 5H, Ar-H), 7.67 (d, 2H, Ar-H, *J*=8.0 Hz), 7.71 (d, 1H, Ar-H, *J*=8.0 Hz), 8.24, 8.36 (2s, 1H, NH, D₂O exchangeable), 8.86, 8.99 (2s, 1H, NH, D₂O exchangeable); Anal. Calcd. for C₂₉H₂₄BrN₅O₄S (618.51): C, 56.32; H, 3.91; N, 11.32; found C, 56.27; H, 3.90; N, 11.28.

4.1.4.18. *4-{3-[4-((5-Bromo-1-(4-cyanobenzyl)-2-oxoindolin-3-ylidene)amino)phenyl]ureido}benzenesulfonamide 9l.*

Yellow orange powder (yield 79%); m.p. over 280 °C; IR (KBr, ν cm^{-1}): 3123-3400 broad band (NH, NH₂), 1714, 1622 (2C=O), 1317, 1159 (SO₂); ¹H NMR (DMSO-*d*₆, 400 MHz) δ ppm: 4.75, 4.79 (2s, 2H, benzylic proton), 6.49 (d, 2H, Ar-H, *J*=8.4 Hz), 6.78 (s, 1H, Ar-H), 6.99 (d, 2H, Ar-H, *J*=8.0 Hz), 7.06 (d, 2H, Ar-H, *J*=8.4 Hz), 7.17 (s, 2H, NH₂, D₂O exchangeable), 7.54 (m, 4H, Ar-H), 7.66 (d, 2H, Ar-H, *J*=8.8 Hz), 7.72 (d, 1H, Ar-H, *J*=8.8 Hz), 8.25 (s, 1H, Ar-H), 9.07 (s, 1H, NH, D₂O exchangeable), 9.15 (s, 1H, NH, D₂O exchangeable).

exchangeable); Anal. Calcd. for $C_{29}H_{21}BrN_6O_4S$ (629.49): C, 55.33; H, 3.36; N, 13.35; found C, 55.22; H, 3.34; N, 13.28.

4.2. Biological Evaluation

4.2.1. CA inhibitory assay

An Applied Photophysics stopped-flow instrument has been used for assaying the CA catalysed CO_2 hydration activity [48]. The inhibition constants were obtained by non-linear least-squares methods using PRISM 3 and the Cheng-Prusoff equation as reported earlier [62-64], and represent the mean from at least three different determinations. The four tested CA isofoms were recombinant ones obtained in-house as reported earlier [65, 66].

4.2.2. Antiproliferative activity against MCF-7 and MDA-MB-231 breast cancer cell lines

Breast cancer MCF-7 and MDA-MB-231 cell lines were obtained from American Type Culture Collection (ATCC). The cells were propagated in DMEM supplemented with 10% heat-inactivated fetal bovine serum, 1% L-glutamine (2.5 mM), HEPES buffer (10 mM), 50 μ g/mL gentamycin and the hypoxia inducer $CoCl_2$ (100 μ M). All cells were maintained at 37 C in a humidified atmosphere with 5% CO_2 . Cytotoxicity was determined following the MTT assay, as reported earlier [50].

4.2.3. Cell cycle analysis

MDA-MB-231 cells were treated with hybrid **6c** for 24 h at its IC_{50} concentration then cells were washed with ice-cold phosphate buffered saline (PBS). The treated cells were collected by centrifugation, fixed in ice-cold 70% (v/v) ethanol, washed with PBS, re-suspended with 100 μ g/mL RNase, stained with 40 μ g/mL PI, and analyzed by flow cytometry using FACS Calibur (Becton Dickinson, BD, USA). The cell cycle distributions were calculated using CellQuest software 5.1 (Becton Dickinson) [26].

4.2.4. Annexin V-FITC apoptosis assay

Phosphatidylserine externalization was assayed using Annexin V-FITC/PI apoptosis detection kit (BD Biosciences, USA) according to the manufacturer's instructions, as reported earlier [67].

4.2.5. VEGFR-2 inhibitory activity assay

VEGFR-2 inhibitory activity was measured for hybrids **6c**, **6d**, **9c** and **9d** using HTScan[®] colorimetric 96-well VEGFR-2 assay kit (catalog no. 7788), according to the manufacturer's protocol as reported earlier [68]. IC₅₀ values were calculated from the concentration–inhibition response curve (triplicate determinations) and the data were compared with sorafenib as a reference VEGFR-2 inhibitor.

Acknowledgements

The authors would like to extend their sincere appreciation to the Deanship of Scientific Research at King Saud University for its funding of this research through the Research Group Project no. RG-1439-65.

References

- [1] C. T. Supuran, Carbonic anhydrases: novel therapeutic applications for inhibitors and activators. *Nat. Rev. Drug Discov.* 7 (2008) 168–181.
- [2] C. T. Supuran, Structure-based drug discovery of carbonic anhydrase inhibitors, *J. Enzyme Inhib. Med. Chem.* 27 (2012) 759–772.
- [3] C.T. Supuran, How many carbonic anhydrase inhibition mechanisms exist? *J. Enzyme Inhib. Med. Chem.* 31 (2016) 345–360.
- [4] (a) C.T. Supuran, Carbonic anhydrase inhibitors and activators for novel therapeutic applications. *Future Med. Chem.* 2011, 3, 1165-1180; (b) E. Masini, F. Carta, A. Scozzafava, C.T. Supuran, Antiglaucoma carbonic anhydrase inhibitors: A patent review. *Expert Opin. Ther. Pat.* 23 (2013) 705–716.
- [5] R. Datta, A. Waheed, G. Bonapace, G. N. Shah, W. S. Sly, Pathogenesis of retinitis pigmentosa associated with apoptosis-inducing mutations in carbonic anhydrase IV *Proc. Natl. Acad. Sci. U.S.A.* 106 (2009) 3437–3442.
- [6] D. Neri, C.T. Supuran, Interfering with pH regulation in tumours as a therapeutic strategy. *Nat. Rev. Drug Discov.* 10 (2011) 767–777.
- [7] S. M. Monti, C.T. Supuran, G. De Simone, Anticancer carbonic anhydrase inhibitors: A patent review (2008–2013). *Expert Opin. Ther. Pat.* 23 (2013) 737–749.

- [8] P. C. McDonald, J. Y. Winum, C. T. Supuran, S. Dedhar, Recent developments in targeting carbonic anhydrase IX for cancer therapeutics, *Oncotarget* 3 (2012) 84–97.
- [9] C.T. Supuran, Carbonic anhydrase inhibition and the management of hypoxic tumors, *Metabolites* 7 (2017) 48.
- [10] Y. Lou, P. C. McDonald, A. Oloumi, S. K. Chia, C. Ostlund, A. Ahmadi, A. Kyle, U. A. Keller, S. Leung, D. G. Huntsman, B. Clarke, B. W. Sutherland, D. Waterhouse, M. B. Bally, C. D. Roskelley, C. M. Overall, A. Minchinton, F. Pacchiano, F. Carta, A. Scozzafava, N. Touisni, J. Y. Winum, C. T. Supuran, S. Dedhar, Targeting tumor hypoxia: suppression of breast tumor growth and metastasis by novel carbonic anhydrase IX inhibitors, *Cancer Res.* 71 (2011) 3364–3376.
- [11] S. M. Monti, C. T. Supuran, G. De Simone, Anticancer carbonic anhydrase inhibitors: a patent review (2008 – 2013), *Expert Opin. Ther. Patents* 23 (2013) 737–749.
- [12] F. E. Lock, P. C. McDonald, Y. Lou, I. Serrano, S. C. Chafe, C. Ostlund, S. Aparicio, J. Y. Winum, C. T. Supuran, S. Dedhar, Targeting carbonic anhydrase IX depletes breast cancer stem cells within the hypoxic niche, *Oncogene* 32 (2013) 5210–5219.
- [13] C. T. Supuran, V. Alterio, A.D. Fiore, K. Ambrosio, F. Carta, S. M. Monti, G. D. Simone, Inhibition of carbonic anhydrase IX targets primary tumors, metastases, and cancer stem cells: Three for the price of one, *Med Res Rev* (2018) 1–38.
- [14] M. Bozdog, M. Ferraroni, E. Nuti, D. Vullo, A. Rossello, F. Carta, A. Scozzafava, C.T. Supuran, Combining the tail and the ring approaches for obtaining potent and isoform-selective carbonic anhydrase inhibitors: solution and X-ray crystallographic studies. *Bioorg. Med. Chem.* 22 (2014) 334–340.
- [15] H. S. Ibrahim, H.A. Allam, W R. Mahmoud, A. Bonardi, A. Nocentini, P. Gratteri, E. S. Ibrahim, H. A. Abdel-Aziz, and C. T. Supuran, Dual-tail arylsulfone-based benzenesulfonamides differently match the hydrophobic and hydrophilic halves of human carbonic anhydrases active sites: Selective inhibitors for the tumor-associated hCA IX isoform, *Eur. J. Med. Chem.* 152 (2018) 1-9.
- [16] M. Fares, R.A. Eladwy, A. Nocentini, S.R.A. El Hadi, H.A. Ghabbour, A. Abdel-Megeed, W.M. Eldehna, H.A. Abdel-Aziz, C.T. Supuran, Synthesis of bulky-tailed sulfonamides incorporating pyrido [2, 3-d][1, 2, 4] triazolo [4, 3-a] pyrimidin-1 (5H)-yl moieties and

evaluation of their carbonic anhydrases I, II, IV and IX inhibitory effects, *Bioorg. Med. Chem.* 25 (2017) 2210-2217

[17] A. Nocentini, M. Ceruso, F. Carta, C.T. Supuran, 7-Aryl-triazolyl-substituted sulfocoumarins are potent, selective inhibitors of the tumor-associated carbonic anhydrase IX and XII, *J. Enzyme Inhib. Med. Chem.* 31 (2016) 1226-1233.

[18] A.M. Alafeefy, R. Ahmad, M. Abdulla, W.M. Eldehna, A.M.S. Al-Tamimi, H.A. Abdel-Aziz, O. Al-Obaid, F. Carta, A.A. Al-Kahtani, C.T. Supuran, Development of certain new 2-substituted-quinazolin-4-yl-aminobenzenesulfonamide as potential antitumor agents, *Eur. J. Med. Chem.* 109 (2016) 247-253.

[19] A. Nocentini, F. Carta, M. Ceruso, G. Bartolucci, C.T. Supuran, Click-tailed coumarins with potent and selective inhibitory action against the tumor-associated carbonic anhydrases IX and XII, *Bioorg. Med. Chem.* 23 (2015) 6955-6966.

[20] M. Bozdog, M. Ferraroni, E. Nuti, D. Vullo, A. Rossello, F. Carta, A. Scozzafava, C. T. Supuran, Combining the tail and the ring approaches for obtaining potent and isoform-selective carbonic anhydrase inhibitors: solution and X-ray crystallographic studies, *Bioorg. Med. Chem.* 22 (2014) 334-340.

[21] A. Medvedev, O. Buneeva, O. Gnedenko, P. Ershov, A. Ivanov, Isatin, an endogenous nonpeptide biofactor: A review of its molecular targets, mechanisms of actions, and their biomedical implications, *Biofactors.* 44 (2018) 95-108.

[22] M. Kidwai, A. Jahan, N.K. Mishra, Isatins: a diversity orientated biological profile, *Med. Chem.* 4 (2014) 451-468.

[23] Goodman VL, Rock EP, Dagher R, et al. Approval summary: sunitinib for the treatment of imatinib refractory or intolerant gastrointestinal stromal tumors and advanced renal cell carcinoma. *Clin Cancer Res* 2007;13:1367-1373.

[24] McCormack PL. Nintedanib: first global approval. *Drugs* 2015;75:129-139.

[25] W.M. Eldehna, H. Almahli, G. H. Al-Ansary, H.A. Ghabbour, M.H. Aly, O. E. Ismael, A. Al-Dhfyhan, and H. A. Abdel-Aziz, Synthesis and in vitro anti-proliferative activity of some novel isatins conjugated with quinazoline/phthalazine hydrazines against triple-negative breast cancer MDA-MB-231 cells as apoptosis-inducing agents, *J. Enzyme Inhib. Med. Chem.* 32, (2017), 600-613.

- [26] W.M. Eldehna, D.H. EL-Naggar, A.R. Hamed, H.S. Ibrahim, H.A. Ghabbour, H.A. Abdel-Aziz One-pot three-component synthesis of novel spirooxindoles with potential cytotoxic activity against triple-negative breast cancer MDAMB-231 cells, *J. Enzyme Inhib. Med. Chem.* 33 (2018) 309-318.
- [27] H.A. Abdel-Aziz, W.M. Eldehna, A.B. Keeton, G.A. Piazza, A.A. Kadi, M.W. Attwa, A.S. Abdelhameed, M.I. Attia, Isatin-benzoazine molecular hybrids as potential antiproliferative agents: synthesis and in vitro pharmacological profiling, *Drug Des. Dev. Ther.*, 11 (2017) 2333-2346.
- [28] H.A. Abdel-Aziz, H.A. Ghabbour, W.M. Eldehna, M.M. Qabeel, H.-K. Fun, Synthesis, Crystal Structure, and Biological Activity of cis/trans Amide Rotomers of (Z)-N'-(2-Oxindolin-3-ylidene)formohydrazide, *Journal of Chemistry*, 2014, Article ID 760434, 7 pages (2014).
- [29] M. El-Naggar, W.M. Eldehna, H. Almahli, A. Elgez, M. Fares, M.M. Elaasser, H.A. Abdel-Aziz, Novel Thiazolidinone/Thiazolo [3, 2-a] Benzimidazolone-Isatin Conjugates as Apoptotic Anti-proliferative Agents Towards Breast Cancer: One-Pot Synthesis and In Vitro Biological Evaluation, *Molecules* 23 (2018) 1420.
- [30] W.M. Eldehna, R.I. Al-Wabli, M.S. Almutairi, A.B. Keeton, G.A. Piazza, H.A. Abdel-Aziz, A.A. Kadi, M.I. Attia, Synthesis and biological evaluation of certain hydrazonoindolin-2-one derivatives as new potent anti-proliferative agents, *J. Enzyme Inhib. Med. Chem.* 33 (2018) 867–878.
- [31] M.F. Abo-Ashour, W.M. Eldehna, A. Nocentini, H.S. Ibrahim, S. Bua, S.M. Abou-Seri, C.T. Supuran, Novel hydrazido benzenesulfonamides-isatin conjugates: Synthesis, carbonic anhydrase inhibitory activity and molecular modeling studies, *Eur. J. Med. Chem.* 157 (2018) 28-36.
- [32] W.M. Eldehna, A. Nocentini, S.T. Al-Rashood, G.S. Hassan, H.M. Alkahtani, A.A. Almehezia, A.M. Reda, H.A. Abdel-Aziz, C.T. Supuran, Tumor-associated carbonic anhydrase isoform IX and XII inhibitory properties of certain isatin-bearing sulfonamides endowed with in vitro anticancer activity towards colon cancer, *Bioorg. Chem.* 81 (2018) 425–432.
- [33] H.S. Ibrahim, S.M. Abou-Seri, M. Tanc, M.M. Elaasser, H.A. Abdel-Aziz, C.T. Supuran, Isatin-pyrazole benzenesulfonamide hybrids potently inhibit tumor-associated carbonic anhydrase isoforms IX and XII, *Eur. J. Med. Chem.* 103 (2015) 583-593.

- [34] O. Güzel-Akdemir, A. Akdemir, N. Karalı, C.T. Supuran, Discovery of novel isatin-based sulfonamides with potent and selective inhibition of the tumor associated carbonic anhydrase isoforms IX and XII, *Org. Biomol. Chem.* 13 (2015) 6493-6499.
- [35] W.M. Eldehna, G.H. Al-Ansary, S. Bua, A. Nocentini, P. Gratteri, A. Altoukhy, H. Ghabbour, H.Y. Ahmed, C.T. Supuran, Novel indolin-2-one-based sulfonamides as carbonic anhydrase inhibitors: synthesis, in vitro biological evaluation against carbonic anhydrases isoforms I, II, IV and VII and molecular docking studies, *Eur. J. Med. Chem.* 127 (2017) 521-530.
- [36] W.M. Eldehna, M.F. Abo-Ashour, A. Nocentini, P. Gratteri, H.I. Eissa, M. Fares, O.E. Ismael, H.A. Ghabbour, M.M. Elaasser, H.A. Abdel-Aziz, C.T. Supuran, Novel 4/3-((4-oxo-5-(2-oxoindolin-3-ylidene) thiazolidin-2-ylidene) amino) benzenesulfonamides: Synthesis, carbonic anhydrase inhibitory activity, anticancer activity and molecular modelling studies, *Eur. J. Med. Chem.* 139 (2017) 250-262.
- [37] W.M. Eldehna, M. Fares, M. Ceruso, H.A. Ghabbour, S.M. Abou-Seri, H.A. Abdel-Aziz, D.A. El Ella, C.T. Supuran, Amido/ureidosubstituted benzenesulfonamides-isatin conjugates as low nanomolar/subnanomolar inhibitors of the tumor-associated carbonic anhydrase isoform XII, *Eur. J. Med. Chem.* 110 (2016) 259-266.
- [38] (a) N. Karalı, A. Akdemir, F. Göktaş, P.E. Elma, A. Angeli, M. Kızılırmak, C.T. Supuran, Novel sulfonamide-containing 2-indolinones that selectively inhibit tumor-associated alpha carbonic anhydrases, *Bioorg. Med. Chem.* 25 (2017) 3714-3718; (b) C. Melis, R. Meleddu, A. Angeli, S. Distinto, G. Bianco, C. Capasso, F. Cottiglia, R. Angius, C.T. Supuran, E. Maccioni, Isatin: a privileged scaffold for the design of carbonic anhydrase inhibitors, *J Enzyme Inhib Med Chem.* 32 (2017) 68-73.
- [39] A. Scozzafava, C. T. Supuran, Carbonic Anhydrase Inhibitor: Ureido and Thioureido Derivatives of Aromatic Sulfonamides Possessing Increased Affinities for Isozymes I. A Novel Route to 2, 5-Disubstituted-1,3,4-Thidiazoles *via* Thioureas and Their Interaction with Isozymes I, II and IV, *J. Enzyme Inhib.* 13 (1998) 103–123.
- [40] J.-Y. Winum, F. Carta, C. Ward, P. Mullen, D. Harrison, S. P. Langdon, A. Cecchi, A. Scozzafava, I. Kunkler, C. T. Supuran, Ureido-substituted sulfamates show potent carbonic anhydrase IX inhibitory and antiproliferative activities against breast cancer cell lines, *Bioorg. Med. Chem. Lett.* 22 (2012) 4681–4685.

- [41] M. Ceruso, S. Antel, D. Vullo, A. Scozzafava, C. T. Supuran, Inhibition studies of new ureido-substituted sulfonamides incorporating a GABA moiety against human carbonic anhydrase isoforms I–XIV, *Bioorg. Med. Chem.* 22 (2014) 6768–6775.
- [42] C. Congiu, V. Onnis, A. Deplano, G. Balboni, M. Ceruso, C. T. Supuran, Synthesis and carbonic anhydrase I, II, IX and XII inhibitory activity of sulfamates incorporating piperazinyl-ureido moieties, *Bioorg. Med. Chem.* 23 (2015) 5619-5625.
- [43] M. Ceruso, S. Antel, A. Scozzafava, C. T. Supuran, synthesis and inhibition potency of novel ureido benzenesulfonamides incorporating GABA as tumor-associated carbonic anhydrase IX and XII inhibitors, *J. Enzyme Inhib. Med. Chem.* 31 (2016) 205-211.
- [44] N. Singasane, P. S. Kharkar, M. Ceruso, C. T. Supuran, M. P. Toraskar, Inhibition of carbonic anhydrase isoforms I, II, IX and XII with Schiff's bases incorporating iminoureido moieties, *J. Enzyme Inhib. Med. Chem.* 30 (2015) 901-907.
- [45] F. Pacchiano, F. Carta, P. C. McDonald, Y. Lou, D. Vullo, A. Scozzafava, S. Dedhar, C. T. Supuran, Ureido-Substituted Benzenesulfonamides Potently Inhibit Carbonic Anhydrase IX and Show Antimetastatic Activity in a Model of Breast Cancer Metastasis, *J. Med. Chem.* 54 (2011) 1896–1902.
- [46] Safety Study of SLC-0111 in Subjects With Advanced Solid Tumours. Available from https://clinicaltrials.gov/ct2/show/study/NCT02215850?term=SLC_0111&rank=1.
- [47] A.S. Smirnov, D.N. Nikolaev, V.V. Gurzhiy, S.N. Smirnov, V.S. Suslonov, A.V. Garabadzhiu, P.B. Davidovich, Conformational stabilization of isatin Schiff bases—biologically active chemical probes, *RSC Adv.* 7 (2017) 10070-10073.
- [48] [31] R.G. Khalifah, The carbon dioxide hydration activity of carbonic anhydrase I. Stop-flow kinetic studies on the native human isoenzymes B and C, *J. Biol. Chem.* 246 (1971) 2561-2573.
- [49] N.K. Tafreshi, M.C. Lloyd, J.B. Proemsey, M.M. Bui, J. Kim, R.J. Gillies, D.L. Morse, Evaluation of CAIX and CAXII Expression in Breast Cancer at Varied O₂ Levels: CAIX is the Superior Surrogate Imaging Biomarker of Tumor Hypoxia, *Mol. Imaging. Biol.* 18 (2016) 219-231.
- [50] T. Mosmann, Rapid colorimetric assay for cellular growth and survival: Application to proliferation and cytotoxicity assays. *J. Immunol. Methods* 65 (1983) 55–63.

- [51] A.M. Rieger, K.L. Nelson, J.D. Konowalchuk, D.R. Barreda, Modified annexin V/propidium iodide apoptosis assay for accurate assessment of cell death, *Journal of visualized experiments: J. Vis. Exp.* 50 (2011) 2597.
- [52] W. Risau, Mechanisms of angiogenesis, *Nature* 386 (1997) 671-674
- [53] K. Holmes, O.L. Roberts, A.M. Thomas, M.J. Cross, Vascular endothelial growth factor receptor-2: structure, function, intracellular signalling and therapeutic inhibition, *Cell. Signal* 19 (2007) 2003-2012.
- [54] W.M. Eldehna, M. Fares, H.S. Ibrahim, M.H. Aly, S. Zada, M.M. Ali, S.M. Abou-Seri, H. A. Abdel-Aziz, D.A.A. El Ella, Indoline ureas as potential anti-hepatocellular carcinoma agents targeting VEGFR-2: Synthesis, *in vitro* biological evaluation and molecular docking. *Eur. J. Med. Chem.* 100 (2015) 89-97.
- [55] A. Nocentini, M. Ferraroni, F. Carta, M. Ceruso, P. Gratteri, C. Lanzi, E. Masini, C.T. Supuran, Benzenesulfonamides incorporating flexible triazole moieties are highly effective carbonic anhydrase inhibitors: synthesis and kinetic, crystallographic, computational, and intraocular pressure lowering investigations, *J. Med. Chem.* 59 (2016) 10692-10704.
- [56] J. Leitans, A. Kazaks, A. Balode, J. Ivanova, R. Zalubovskis, C.T. Supuran, K. Tars, Efficient expression and crystallization system of cancer-associated carbonic anhydrase isoform IX, *J. Med. Chem.* 58 (2015) 9004-9009.
- [57] W.M. Eldehna, M. Fares, H.S. Ibrahim, M.A. Alsherbiny, M.H. Aly, H.A. Ghabbour and H.A. Abdel-Aziz, Synthesis and Cytotoxic Activity of Biphenylurea Derivatives Containing Indolin-2-one Moieties, *Molecules*, 21 (2016), p.762.
- [58] W.M. Eldehna, M.F. Abo-Ashour, H.S. Ibrahim, G.H. Al-Ansary, H.A. Ghabbour, M.M. Elaasser, H. YA Ahmed, N.A. Safwat, Novel [(3-indolylmethylene) hydrazono] indolin-2-ones as apoptotic anti-proliferative agents: design, synthesis and *in vitro* biological evaluation, *J. Enzyme Inhib. Med. Chem.* 33, (2018), 686-700.
- [59] M.I. Attia, W.M. Eldehna, S.A. Afifi, A.B. Keeton, G.A. Piazza, H.A. Abdel-Aziz, New hydrazonoindolin-2-ones: Synthesis, exploration of the possible anti-proliferative mechanism of action and encapsulation into PLGA microspheres, *PloS one*, 12 (2017) e0181241.
- [60] K.R. Senwar, P. Sharma, T.S. Reddy, M.K. Jeengar, V. L. Nayak, V.G.M. Naidu, A. Kamal, N. Shankaraiah, Spirooxindole-derived morpholine-fused-1, 2, 3-triazoles: Design, synthesis, cytotoxicity and apoptosis inducing studies, *Eur. J. Med. Chem.* 102 (2015) 413-424.

- [61] M. Damgaard, A. Al-Khawaja, S.B. Vogensen, A. Jurik, M. Sijm, M. EK Lie, M. I. Bæk E. Rosenthal, A.A. Jensen, G.F. Ecke, B. Frølund, P. Wellendorph, R.P. Clausen, Identification of the first highly subtype-selective inhibitor of human GABA transporter GAT3, *ACS Chem. Neurosci.* 6 (2015) 1591-1599.
- [62] A. Nocentini, M. Ceruso, S. Bua, C.L. Lomelino, J.T. Andring, R. McKenna, C. Lanzi, S. Sgambellone, R. Pecori, R. Matucci, L. Filippi, P. Gratteri, F. Carta, E. Masini, S. Selleri, C.T. Supuran. Discovery of β -Adrenergic Receptors Blocker-Carbonic Anhydrase Inhibitor Hybrids for Multitargeted Antiglaucoma Therapy. *J. Med. Chem.* 61 (2018) 5380-5394.
- [63] A. Nocentini, F. Carta, M. Tanc, S. Selleri, C.T. Supuran, C. Bazzicalupi, P. Gratteri. Deciphering the Mechanism of Human Carbonic Anhydrases Inhibition with Sulfo coumarins: Computational and Experimental Studies. *Chemistry.* 24 (2018) 7840-7844.
- [64] A.A. Abdel-Aziz, A.S. El-Azab, M.A. Abu El-Enin, A.A. Almehezia, C.T. Supuran, Nocentini A. Synthesis of novel isoindoline-1,3-dione-based oximes and benzenesulfonamide hydrazones as selective inhibitors of the tumor-associated carbonic anhydrase IX. *Bioorg. Chem.* 80 (2018) 706-713.
- [65] A. Nocentini, S. Bua, C.L. Lomelino, R. McKenna, M. Menicatti, G. Bartolucci, B. Tenci, L. Di Cesare Mannelli, C. Ghelardini, P. Gratteri, C.T. Supuran. Discovery of New Sulfonamide Carbonic Anhydrase IX Inhibitors Incorporating Nitrogenous Bases. *ACS Med. Chem. Lett.* 8 (2017) 1314-1319.
- [66] A. Nocentini, R. Cadoni, P. Dumy, C.T. Supuran, J.Y. Winum. Carbonic anhydrases from *Trypanosoma cruzi* and *Leishmania donovani chagasi* are inhibited by benzoxaboroles. *J. Enzyme Inhib. Med. Chem.* 33 (2018) 286-289.
- [67] H.A. Abdel-Aziz, W.M. Eldehna, H. Ghabbour, G.H. Al-Ansary, A.M. Assaf, A. Al-Dhfyhan, Synthesis, crystal study, and anti-proliferative activity of some 2-benzimidazolylthioacetophenones towards triple-negative breast cancer MDA-MB-468 cells as apoptosis-inducing agents, *Int. J. Mol. Sci.* 17 (2016) 1221.
- [68] W.M. Eldehna, S.M. Abou-Seri, A.M. El Kerdawy, R.R. Ayyad, A.M. Hamdy, H.A. Ghabbour, M.M. Ali, D.A. Abou El Ella, Increasing the binding affinity of VEGFR-2 inhibitors by extending their hydrophobic interaction with the active site: design, synthesis and biological evaluation of 1-substituted-4-(4-methoxybenzyl) phthalazine derivatives, *Eur. J. Med. Chem.* 113 (2016) 50-62.

Highlights

- Two novel *N*-substituted isatins-SLC-0111 hybrids series (**6a-f** and **9a-l**) were developed.
- As planned, a substantial improvement of inhibitory profile towards hCA IX was achieved.
- Docking unveiled accommodation of *N*-alkylated isatin moieties in a wide hydrophobic pocket.
- Both hCA IX and XII were efficiently inhibited (K_{iS} : 4.7–86.1 and 1.3–80.9 nM, respectively).
- Antitumor, cell cycle disturbance and pro-apoptotic activities were evaluated in breast cancer.
- Hybrids **6c**, **6d**, **9c** and **9d** displayed good VEGFR-2 inhibitory activity (IC_{50} : 207 – 462 nM).